Biosensors and Bioelectronics 76 (2016) 195–212

Contents lists available at ScienceDirect

Biosensors and Bioelectronics

journal homepage: www.elsevier.com/locate/bios

Recent advances in electrochemical biosensors based on graphene two-dimensional nanomaterials

Yang Song [a,b], Yanan Luo [a,b], Chengzhou Zhu [b], He Li [b], Dan Du [a,b,c,*], Yuehe Lin [a,b,c,*]

[a] Key Laboratory of Pesticide and Chemical Biology of Ministry of Education, College of Chemistry, Central China Normal University, Wuhan, PR China
[b] Department of Mechanical and Material Engineering, Washington State University, Pullman, WA 99164, United States
[c] Paul G. Allen School for Global Animal Health, Washington State University, Pullman, WA 99164, United States

ARTICLE INFO

Article history:
Received 27 April 2015
Received in revised form
19 June 2015
Accepted 2 July 2015
Available online 5 July 2015

Keywords:
Two-dimensional nanomaterials
Graphene
Electrochemical biosensor
Enzyme-based biosensors
DNA sensors
Immunosensors

ABSTRACT

Graphene as a star among two-dimensional nanomaterials has attracted tremendous research interest in the field of electrochemistry due to their intrinsic properties, including the electronic, optical, and mechanical properties associated with their planar structure. The marriage of graphene and electrochemical biosensors has created many ingenious biosensing strategies for applications in the areas of clinical diagnosis and food safety. This review provides a comprehensive overview of the recent advances in the development of graphene based electrochemical biosensors. Special attention is paid to graphene-based enzyme biosensors, immunosensors, and DNA biosensors. Future perspectives on high-performance graphene-based electrochemical biosensors are also discussed.

1. Introduction

Two-dimensional (2D) nanomaterials have been employed in recent years to develop biosensing devices because of their special electronic, optical and mechanical properties (Chen and Chatterjee, 2013; Putzbach and Ronkainen, 2013; Pumera, 2012, 2010). Specifically, among the reported 2D nanomaterials, graphene has emerged as the most powerful nanomaterial for diverse applications (Chen et al., 2015). Graphene refers to a sheet of sp^2-bonded carbon atoms arranged into a rigid honeycomb lattice, exhibiting one of the highest mechanical strength among all materials, extraordinary electron transfer capability and excellent thermal conductivity (Lawal, 2015; Goenka et al., 2014; Liu et al., 2012c; Premkumar and Geckeler, 2012; Nguyen and Berry, 2012; Xiang et al., 2012; Pumera et al., 2010; Dresselhaus and Araujo, 2010; Geim, 2009; Li and Kaner, 2008). Due to its tremendous unique properties, graphene holds great promise for a broad range of applications, such as energy storage (*e.g.* fuel cells, batteries and supercapacitors) and biological applications. Its high specific surface area and the ease of functionalizing its surface can accommodate highly active probes and targets of interest, which is favorable for developing a novel bio-interface for biosensing (Vashist and Luong, 2015; Ping et al., 2015; Fang and Wang, 2013; Liu et al., 2012c; Pumera, 2010). Moreover, the recently successful synthesis of graphene nanosheets via various protocols and the integration of graphene with different nanomaterials, such as metals, metal oxides, and quantum dots, could provide abundant opportunities for developing novel biosensors with enhanced performance (Mao et al., 2013). An attractive synergy effect could be obtained accordingly. For example, graphene can be decorated with metal nanoparticles (NPs) to achieve a notable increase in electron transfer rate when it is applied on an electrical device, resulting the significant improved performance of electrochemical biosensors (Ambrosi et al., 2014; Walcarius et al., 2013; Du et al., 2012; Kamat, 2010). Recent frontier research on the rational design of functional graphene nanocomposites, coupled with electrochemical analytic methods, has led to advances in electrochemical applications. Among these works, graphene have been used to analyze various inorganic and organic analytes in the biomedical and environment applications, including glucose (Shan et al., 2010), cysteine (Wu et al., 2012), proteins (Lu et al., 2012), biomarkers (Yang et al., 2011a), DNA (Premkumar and Geckeler, 2012; Lv et al., 2010), heavy metal (Wang et al., 2011a), etc. Our group has synthesized a series of graphene-based nanomaterials that have been used to develop and fabricate advanced biosensors with promising performance for bioanalytical applications (Wang et al., 2014d, 2010; Tang et al., 2010).

* Corresponding authors at: Central China Normal University, Key Laboratory of Pesticide & Chemical Biology of Ministry of Education, Wuhan, Hubei Province 430079, China.
E-mail addresses: dan.du@mail.ccnu.edu.cn (D. Du), yuehe.lin@wsu.edu (Y. Lin).

http://dx.doi.org/10.1016/j.bios.2015.07.002
0956-5663/

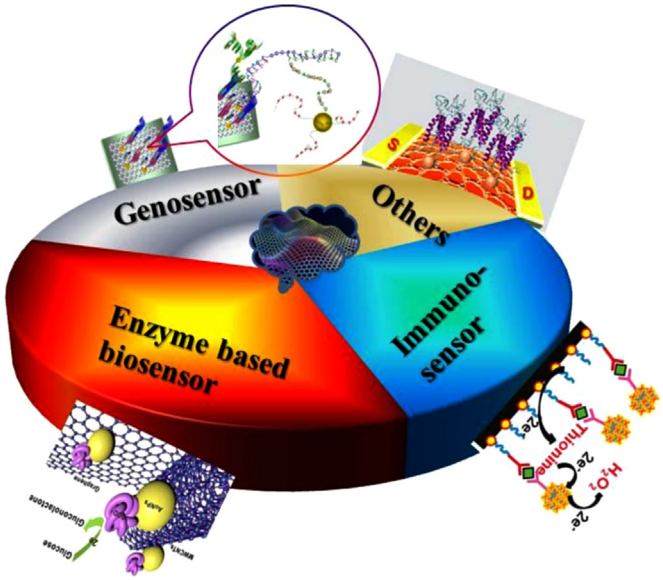

Scheme 1. Schematic illustration of electrochemical biosensors based on graphene nanomaterial, in which enzyme-based biosensors, genosensors and immunosensors, are demonstrated.

This review summarizes recent advances in electrochemical biosensors based on graphene based nanomaterials over the past three years. Enzyme-based biosensors, genosensors, and immunosensors are then mainly discussed (Scheme 1). In addition, we also point out the challenges and future perspectives related to the material design and development of graphene-based biosensor.

2. Granphene-based electrochemical enzymatic biosensors

2.1. Graphene-based electrochemical enzymatic biosensors for glucose detection

The third generation of glucose biosensors, which takes advantage of direct electron transfer (DET) in enzymatic reaction catalysis, has been intensively studied for decades and continues to be developed (Wang and Yao, 2012). The direct electrochemistry of glucose oxidase (GOx) refers to DET between the electrode surface and the enzyme active site in the absence of a mediator. Recently, graphene hybrid with various nanomaterials, such as metal chalcogenides (Yu et al., 2014a; Ramakrishna Matte et al., 2010), metal oxides (Dong et al., 2012a), and polymer (Salavagione et al., 2011), were prepared and investigated as the third generation of glucose biosensors. Electrons cross the long tunneling distance through enzymes, thereby achieving direct GOx electrochemistry on graphene-modified electrodes (Zhang et al., 2015a, 2014d; Bai et al., 2013b, 2012; Huang et al., 2013a; Gu et al., 2012; Liu et al., 2011; Zhou et al., 2010). The favorable electron transfer kinetics and high sensitivity are originated from the good conductivity and large surface area of graphene favoring for immobilization of GOx. The use of electrochemically reduced graphene has been reported for the construction of a glucose biosensor using the same strategy (Liang et al., 2013). In this work, the unique graphene nanostructures were fabricated by electrochemical reduction. The conductivity of graphene was significantly meliorated when the oxygen-containing groups were eliminated during the reduction reaction. The carboxylic acid groups remained to immobilize GOx. One pair of well-defined redox peaks was obtained.

Graphene quantum dots (GQDs) are a successful example of a graphene nanomaterial that is used to construct novel electrochemical sensors (Razmi and Mohammad-Rezaei, 2013). The process refers to the modification of GQDs and the surface immobilization of GOx, which results in a wide linear glucose response (5–1270 μM), low detection limit (1.73 μM) and high surface coverage of GOx (1.8×10^{-9} mol cm^{-2}). The resulting DET is attributed to the large surface-to-volume ratio, excellent biocompatibility and abundant hydrophilic edges and planes of GQDs, which enhance the enzyme immobilization on the electrode surface. In a pioneering work, mesocellular graphene foam (MGF) was easily synthesized and conveniently used for the immobilization and direct electrochemistry of GOx. A continuous crystal lattice was observed throughout the mesoporous network, and the porous nanostructure exhibited high conductivity, an ultra-large surface area (2581 m^2 g^{-1}), and high pore volume (5.53 cm^3 g^{-1}) and facilitated electron transfer (Wang et al., 2014c). In another report, a fiber-like graphene nanostructure was easily created through homogeneous dispersion with polyaniline (PANI) through ultrasonication (Xu et al., 2014). The homogeneous dispersion of graphene and PANI yielded a fiber-like structure that effectively encapsulated GOx. A reversible redox process of GOx was observed. This type of biosensor exhibited a high amount of GOx loading on graphene electrodes and a remarkably heightened electron transfer rate, 2.6 s^{-1}. Generally, the large surface-to-volume ratio of graphene contributes to high amounts of GOx loading (Yang et al., 2013f; Zhu et al., 2010; Geim, 2009). Moreover, a series of specific graphene nanomaterials, including graphene/chitosan, graphene/carbon nanotube (CNT), graphene/ion liquid and graphene/Nafion, offer great opportunities to create more complexly functional nanostructures and novel glucose biosensors (Li et al., 2015; Cao et al., 2013b; Hui et al., 2013; Chen et al., 2012c; Zhang et al., 2011).

The integration of polymers with graphene has been intensively investigated because it improves the sensitivity of glucose biosensor due to its unique structural and compositional sophistication of the nanocomposites. (Park et al., 2015; Ruan et al., 2013; Claussen et al., 2012). In comparison with other graphene-based nanomaterials, the large surface area endows polymer-dispersed graphene with enhanced mass transport and high GOx loading. Chitosan, which is a unique class of inorganic polymer with low density, high porosity, high surface area, and superior physical and chemical properties, is often combined with graphene to obtain a functional nanostructure for enhancing the performance of glucose biosensors (Liu et al., 2015b; Song et al., 2014; Zhong et al., 2012). Currently, Kang et al. (2009) reported a pioneering work on utilizing graphene–chitosan nanocomposite film to fabricate glucose biosensors, providing stable dispersion of graphene and a large range of functionalities. The favorable nanostructure accelerated the heterogeneous electron transfer between the electrode surface and GOx, yielding a rate of 2.83 s^{-1}. This glucose biosensor also exhibited a broad linear glucose response from 0.08 to 12 mM, with detection limit as low as 0.02 mM. Other polymers were also explored to incorporate with graphene nanomaterial, endowing the new functionalities of graphene/polymer nanocomposites. The creation of polymer-capped graphene nanocomposites using poly(diallyldimethylammonium chloride) (PDDA) as the electrode material has aroused significant attention (Yu et al., 2014b). GOx was immobilized on the surface of modified electrodes through strong electrostatic interaction (Fig. 1). The unique microstructure exhibited highly specific electrocatalytic activities toward glucose in the presence of ascorbic acid (AA) and uric acid (UA). Kong et al. (2014) successfully developed an easy to use and sensitive glucose biosensor based on graphene@PANI nanocomposite along with the covalent adsorption of GOx on a screen-printed carbon electrode (SPCE). The nanocomposites are extremely high in porosity, yielding a fantastic

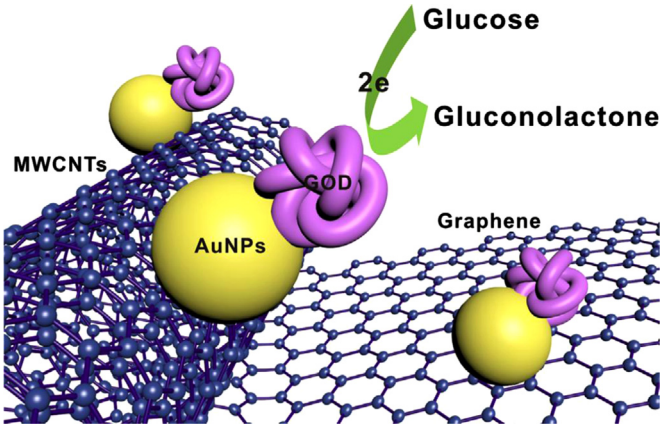

Fig. 1. Schematic illustration of construction of GOD/Au NPs/G/MWCNTs nanocomposites, in which polymer capped graphene nanostructure was used to immobilize GOx and homogeneously load Au NPs. Reproduced from Yu et al. (2014b) by permission of Elsevier Science Ltd.

surface structure on the nanometer scale. The current signal during GOx-glucose reaction was measured using differential pulse voltammetry (DPV). This enzyme-modified SPCE coupled with a paper disk enables glucose determination with lower volumes of reagents and samples and an easier operation procedure in comparison with traditional methods, holding great promise for glucose analysis in commercial areas (Fig. 2).

In addition, another attractive approach to the construction of glucose biosensors was to harness graphene's properties through incorporation with various functional materials, such as metal/metal oxide/metal chalcogenide NPs. The introduction of these functional materials attracted great attention because of the synergistic contribution to enhancing the conductivity and accelerating electron transfer, thus improving the electrochemical performance in glucose biosensing. As a pioneering work, Kavitha et al. (2012) successfully fabricated a uniform graphene–ZnO nanosheet to establish a biosensing platform for achieving DET of GOx. The graphene–ZnO nanosheet was synthesized by the *in situ* generation of ZnO NPs onto graphene at relatively low temperature. The graphene/ZnO nanosheets display high surface areas and excellent electrical conductivity. Native enzyme configuration was realized on the electrode surface and DET was achieved between activity site of GOx and the electrode surface. Jang et al. (2012) illustrated the synthesized TiO_2-graphene nanocomposite electrode for enzyme capture, on which DET of GOx was efficiently achieved. The results showed that TiO_2 NPs were encapsulated into graphene nanosheets and the morphology of TiO_2-graphene nanocomposites was spherical structure. TiO_2 NPs exhibited strikingly high biocompatibility for GOx. A high current response for glucose up to 8 mM was observed. Wang et al. (2011b) succeeded in immobilizing GOx in a mixture containing graphene and CdS nanocomposites. The excellent biocompatibility of the graphene–CdS matrix and its special physicochemical properties were favorable for high sensitivity. The presence of CdS nanocrystal in the graphene-based matrix not only offered a biocompatible microstructure but also accelerated electron transfer between the active site of the enzyme and the electrode surface. Recently, a series of graphene/metal NPs based biosensors were also advocated to exploit the synergistic effect of graphene and metal NPs (*e.g.* Au NPs (Shan et al., 2010), Pt NPs (Wu et al., 2009), Pd NPs (Lu et al., 2011a; Zeng et al., 2011), and Ag NPs (Lu et al., 2011b)) to enhance electron transfer in glucose determination. It is anticipated that graphene/metal based NPs will not only pave a new route to host enzyme for developing enzyme based biosensor but also broaden other electrochemical applications.

Though all of the previous studies achieved well-defined redox peaks for the direct electrochemistry of GOx, the hypostasis of DET of GOx on glucose determination has not been clearly investigated because of the presence of oxygen. The third generation of glucose biosensor is rigorously oxygen exclusive whereas the first generation amperometric glucose biosensor is not. To clarify this problem, Liang et al. (2015) systematically investigated the signal transduction of DET and enzyme activity in glucose biosensor based on GOx self-assembled on the graphene modified electrode. The evidence of DET of GOx in glucose detection on the GOx-graphene hybrid-modified electrode, two well-defined redox peaks of direct GOx electrochemistry, was obtained. The reactions related to the electrochemical determination of glucose and the enzymatic activities of GOx on the graphene modified electrodes were fully investigated. However, as those GOx molecules participating in DET lacked enzymatic activity toward glucose, DET cannot be identified as the essential mechanism point of glucose determination in GOx-graphene based biosensors. With oxygen consumption due to the mediated enzymatic oxidation of glucose, the biosensor can perform sensitive detection of glucose in an air-saturated solution. The remarkable enhancement of redox peaks relies on the net drop in biosensor current ascribed to the decrease in O_2 reduction current and increase in H_2O_2 reduction current. Moreover, GOx adsorbed on a graphene surface was hardly able to maintain the enzyme activity in a biosensor, which indicated that graphene would significantly decrease the average enzymatic activity of GOx (Fig. 3). A similar loss of enzyme activity of GOx adsorbed on nanomaterial-modified surfaces, such as CNT (Wooten et al., 2014; Goran et al., 2013; Liang et al., 2013) and Au NPs

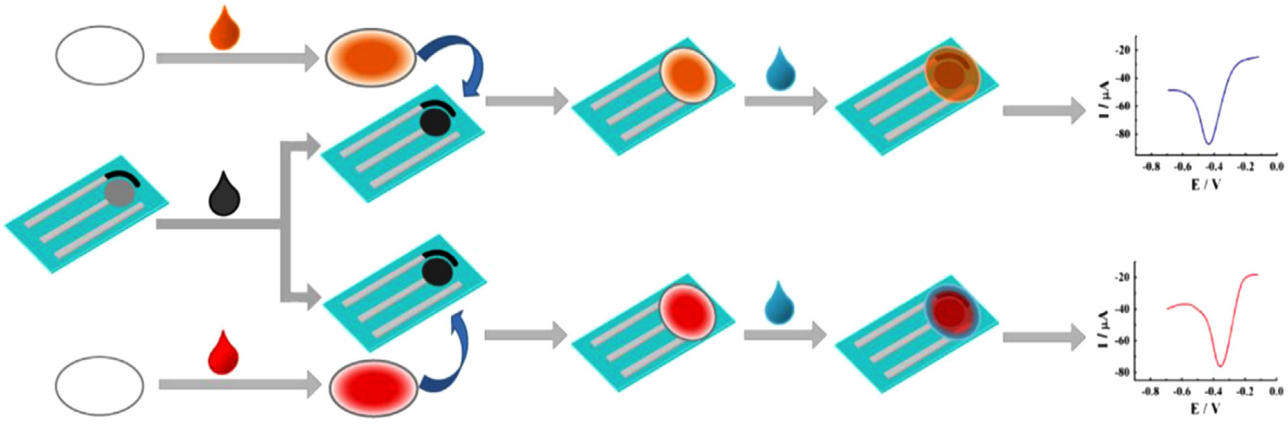

Fig. 2. Schematic representation of the fabrication and assay procedure of the paper-based glucose biosensor. Reproduced from Kong et al. (2014) by permission of Elsevier Science Ltd.

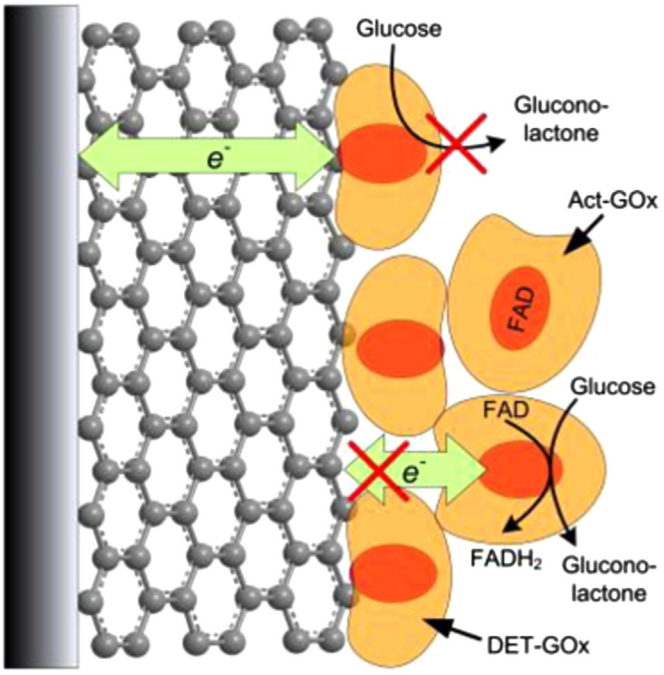

Fig. 3. Schematic illustration of GOx adsorbed on the surface of electroreduced graphene oxide (ERGO) modified GCE. Reproduced from Liang et al. (2015) by permission of Elsevier Science Ltd.

(Seehuber and Dahint, 2013), have also been reported previously (Table 1).

2.2. Graphene-based electrochemical enzymatic biosensors for hydrogen peroxide detection

Considerable attention has been aroused in recent decades in the rapid and accurate quantitative detection of H_2O_2, which has practical uses in chemical and biological analysis and in clinical diagnostics and environmental protection. Recently, graphene nanomaterials have played a pivotal role as a key part of electrochemical biosensor systems because of their promising performance and superior analytical principles to other conventional types. Specifically, graphene's large surface area and high conductivity can produce a synergistic effect between catalytic activity and biocompatibility. A wide variety of graphene-based electrochemical biosensors have been explored in H_2O_2 detection. For example, as shown in Fig. 4, graphene capsule, which served as carrier for HRP, was designed to detect H_2O_2 in human serum. Compared with other reports, the results exhibited fair stability, reproducibility and good selectivity under interference, indicating promising potential for medical analysis (Fan et al., 2015). A supermolecular assembly enzymatic functional graphene-based biosensor was fabricated using HRP/cyclodextrin to detect H_2O_2 (Lu et al., 2013). The adamantine-modified HRP interacted with functionalized graphene nanostructures in aqueous solution by host-guest supramolecular chemistry, which improved the electrochemical performance for H_2O_2 detection. They found that the functionalized graphene nanostructures exhibited better conductivity and faster electron rate in comparison to the original graphene nanosheets. This innovative nanostructure presented excellent performance in catalytic applications in clinical diagnostics, environmental monitoring and other biosensing areas. An enzymatic electrochemical biosensor based on a graphene nanoplatelet–titanate nanotube composite was designed and synthesized by a hydrothermal method and exhibited sensitive H_2O_2 detection in a relatively wide potential range, with a high recovery rate compared with previous sensors (Liu et al., 2014b). A convenient and extremely high-sensitivity electrochemical enzymatic detection platform for H_2O_2 was fabricated on a glass carbon electrode (GCE) through HRP peptide amide bonding with GQDs immobilized onto the electrode surface (Muthurasu and Ganesh, 2014). The GQD-modified electrode was utilized as a biocompatible platform for HRP immobilization, yielding a HRP/GQD biosensor with good electrocatalytic performance toward H_2O_2. The detection range is 1.0–100 μM with the detection limit down to

Table 1
Graphene-based glucose biosensors.

Graphene modified electrode	Linear range (LOD)	Sensitivity	Reference
Graphene platelet/GOx	2–22 mM	20 μM	Liu et al. (2011)
Reduce graphene/GOx/Nafion	10–500 μM	3.33 μM	Gu et al. (2012)
Reduce graphene sheet/GOx	1–10 mM	100 μM	Zhang et al. (2014d)
GQDs/GOx	5–1270 μM	1.73 μM	Razmi and Mohammad-Rezaei (2013)
Reduced carboxyl graphene/GOx	2–18 mM	0.02 mM	Liang et al. (2013)
MGF/GOx	1–12 mM	0.25 mM	Wang et al. (2014c)
Graphene/PANI/Au NPs/GOx	0.004–1.12 mM	0.6 μM	Xu et al. (2014)
Polymeric ionic liquid/graphene/GOx	0.8–20 mM	0.267 mM	Zhang et al. (2011)
Graphene/CNT/GOx	1–8 mM	1 mM	Chen et al. (2012c)
Graphene/Nafion/GOx	2–14 mM	0.04 mM	Hui et al. (2013)
Graphene/Au NPs/GOx	0.02–2.26 mM	4.1 μM	Cao et al. (2013b)
Polydopamine/Graphene/GOx	0.001–4.7 mM	0.1 μM	Ruan et al. (2013)
C-PPy/Graphene/GOx	1–100 μM	1 nM	Park et al. (2015)
Polymer/Graphene/Pt NPs	0.01–50 mM	0.03 μM	Claussen et al. (2012)
Chitosan/Prussian blue/graphene/GOx	0.025–3.2 mM	0.01 mM	Zhong et al. (2012)
Chitosan/Reduced Graphene/GOx	1–10 mM	0.1 mM	Song et al. (2014)
Graphene/Chitosan/GOx	0.08–12 mM	0.02 mM	Kang et al. (2009)
Graphene/PDDA/GOx	0.3–2.1 mM	4.8 μM	Yu et al. (2014b)
Graphene/PANI/Au NPs/GOx	0.2–11.2 μM	0.1 μM	Kong et al. (2014)
Graphene/ZnO/GOx	1–10 mM	0.1 mM	Kavitha et al. (2012)
Graphene/TiO_2/GOx	0.1–8 mM	10 μM	Jang et al. (2012)
Graphene/CdS/GOx	2–16 mM	0.7 mM	Wang et al. (2011b)
Graphene/Au NPs/chitosan/GOx	0.2–4.2 mM	0.18 mM	Shan et al. (2010)
Graphene/Pt/chitosan/GOx	0.15–4.2 mM	0.6 μM	Wu et al. (2009)
Graphene/Pd/Nafion/GOx	0.01–5 mM	1 μM	Lu et al. (2011a)
Graphene/Pd/chitosan/GOx	0.001–1.0 mM	0.2 μM	Zeng et al. (2011)
Graphene/SiO_2/Ag NPs/GOx	0.1–0.26 M	4 μM	Lu et al. (2011b)

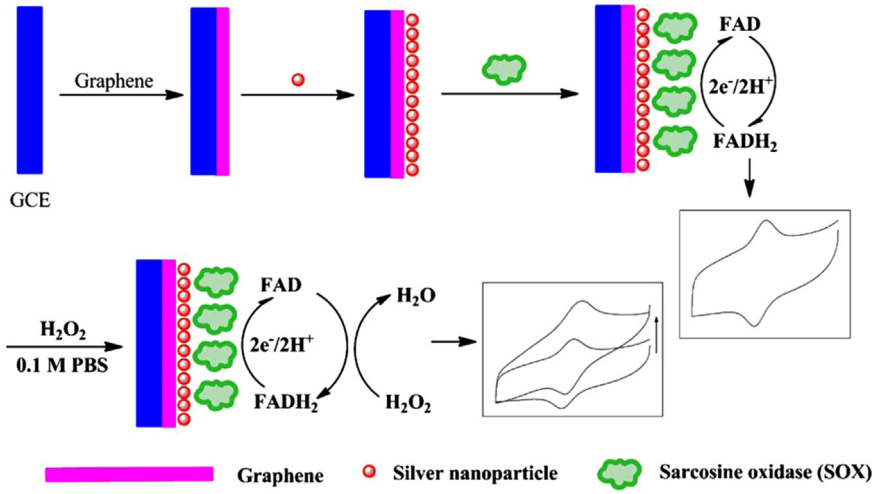

Fig. 4. Schematic diagrams for the biosensor fabrication and determination of H_2O_2. Reproduced from Zhou et al. (2012b) by permission of Elsevier Science Ltd.

530 nM.

Furthermore, noble metals are considered promising electrochemical candidates to improve the performance of electrochemical applications because of their synergistic effects. A H_2O_2 biosensor was investigated based on DET of sarcosine oxidase on a graphene–chitosan–Ag NP-modified electrode (Zhou et al., 2012b). The high sensitivity originates from DET of the enzyme, resulting from the large specific surface area and good conductivity of graphene nanomaterials. Layer-by-layer assembly of hemoglobin-Au NPs with graphene-modified electrodes was employed to design a sensitive and selective H_2O_2 biosensor. The Au–graphene nanocomposites can be used as a biocompatible matrix for HRP immobilization and can yield a HRP/Au/graphene biosensor with high sensitivity and precise detection of H_2O_2 in human serum and with great potential for the direct electrochemical detection of different analytes (Zhang et al., 2014b). On this basis, graphene conjugated with flower-like ZnO and Au NPs was also fabricated to develop a H_2O_2 biosensor (Xie et al., 2013). These nanocomposites combined with hemoglobin served as an effective biosensing platform exhibiting fast response toward H_2O_2 with good sensitivity and a wide linear response range.

2.3. Graphene-based electrochemical enzymatic biosensors for NADH detection

NADH, which is an important coenzyme in all living cells and a redox carrier in metabolic processes, participates in several hundred enzymatic reactions. The electrochemical oxidation of NADH often involves the fabrication of dehydrogenase-based biosensors. Recently, graphene-based electrochemical biosensors have been developed that achieve excellent electrocatalytic activity toward NADH (Gasnier et al., 2013; Teymourian et al., 2013). The graphene-induced self-assembly of peptide nanowires has been used to develop an electrochemical biosensor for NADH and enhance the electronic conductivity of the bio-structure remarkably (Li et al., 2013b). This graphene-based NADH biosensor displayed high sensitivity, thereby holding great promise for the NADH analysis in various fields. An electrochemical NADH biosensor fabricated with a graphene paste electrode has been employed to selectively catalyze the electrooxidation of different analytes, including NADH, without any interference by surface passivation (Gasnier et al., 2013). This biosensor outperformed other electrochemical NADH biosensors because it integrated the excellent electrocatalytic activities of graphene, its unique properties in interacting and incorporating with biomolecules and its short preparation time successfully.

Conductive polymer-modified electrodes have been applied in biosensors for many years. A NADH biosensor has used the electrodeposition of ERGO and polythionine (PTH) on a GCE to form a nanocomposite film (Li et al., 2013c). This nanocomposite film was applied as a transducer to improve the electrocatalytic oxidation of NADH and also used to construct a dehydrogenase-based amperometric biosensor. The synergistic effect of this nanostructure could enhance the electrocatalytic activity for detection.

Gai et al. (2014) developed a novel electrochemical NADH biosensor using N-doped graphene. N-doped graphene exhibited highly similar properties to NADH dehydrogenase and thus efficiently catalyzed NADH oxidation. In addition, N-doped graphene served as a DET shuttle from NADH to the electrode surface because of its extremely high conductivity. With low background current, this graphene material improved the selectivity and sensitivity of the biosensor for NADH determination.

2.4. Other interests

Several novel electrochemical detection protocols and strategies based on graphene have been advanced for other enzyme-based biosensors during this past three years. Sun et al. (2013) reported a graphene and TiO_2 nanorods modified electrode for direct electrochemistry of hemoglobin, one important substance for transporting oxygen in blood. Typically, hemoglobin was immobilized in the graphene–TiO_2 nanocomposite to improve electron transfer rate between active site of hemoglobin and the substrate electrode. This biosensor exhibited excellent electrocatalytic activity for the reduction of trichloroacetic acid in the concentration range from 0.6 to 20 mM. Using these advantages, a high sensitive nitric oxide (NO) biosensor was introduced based on hemoglobin, achieving quantitative measurements of NO concentration to overcome the disadvantages of existed NO biosensor (Wen et al., 2012). Hemoglobin was immobilized in the chitosan–graphene and surfactant hexadecytrimethylammonium bromide nanocomposite on electrode surface, which was utilized to quantitatively measure NO. A graphene–copper sulfide nanocomposite modified electrode was utilized for electrochemical analysis of hemoglobin. Graphene and copper sulfide nanocomposite was synthesized by hydrothermal method. Hemoglobin was immobilized on the electrode surface to obtain this biocompatible biosensing platform (Shi et al., 2015). DET of hemoglobin and enhanced electron transfer were realized. The enzyme kinetics was also analyzed to accurately measure the kinetic constant. This

electrochemical assay could also be used to analyze varieties of interests. Jiang et al. (2014) reported graphene–gold hybrids on electrochemical detection of nitrite. Through the optimization of the arrangement of graphene–gold hybrids and the hemoglobin, this biosensing architecture exhibited a superior output signal performance with a low detection limit down to 10 nM. Chen et al. (2012a) summarized abundant different methods of graphene oxides (GO) fabrication with desirable and specific nanostructure along with the technology of electrodes modification for electrochemical biosensor. In the past two years, several researches successfully extended to GO in the exploration of different kinds of electrochemical biosensors. In a typical GO based electrochemical biosensing system, GO was combined with Au nanocluster by sonication to modify electrode surface (Ge et al., 2012). Then L-cysteine could be oxidized on the GO modified electrode. This direct determination of free reduced L-cysteine in real samples has achieved abroad linear detection range from 0.05 to 20 μM and an extremely low detection limit of 0.02 μM without distinct interference from metal ions, nucleotide acid and amino acids. In another work, a GO-graphene based functionalized nanocomposite was developed for the determination of herbicide diuron (Sharma et al., 2013). By *in-situ* electrochemical synthesis approach, GO-graphene exhibited electrical and chemical synergies for developing biocompatible immunosensing platform, resulting in increasing in electrochemical signal response for diuron determination. Wu et al. (2012) developed an electrochemical biosensor for selective cysteine detection in serum based on a functional graphene nanoribbon (GNR) and Nafion nanocomposites. They found that the presence of GNR enhances the electrochemical oxidation of cysteine and thus, improves the sensitivity of biosensor, opening a promising use of these materials in nano-level electrochemical detection.

Electrochemical cytochrome c biosensor is also receiving increasing research attention due to its unique biological properties. Considerable efforts have been made to expand the design of this assay with graphene modified electrodes because of the increasing concern of direct electrochemistry of cytochrome c (Yang et al., 2013a). A novel bi-protein interphase of cytochrome c and GOx on graphene modified electrode was claimed to achieve DET between proteins and electrode with wide linear response range and low detection limit (Song et al., 2013b). Bi-protein integrated with PDDA/graphene/Au NPs nanocomposites accelerated electron transfer via cytochrome c toward electrode. Zhang et al. (2013) took the advantage of perylene to synthesize perylene–graphene matrix with good biocompatibility. The resulting composite was more favorable for immobilization of cytochrome c and DET of cytochrome c can be easily achieved on the constructed biointerface. At the same time, this cytochrome c modified biointerface showed enhanced electrocatalytic activity toward H_2O_2 reduction with detection limit down to 3.5 μM. In another work, graphene nanosheets-Au NPs hybrid nanocomposites were fabricated under hydrothermal condition, which was used to encapsulate cytochrome c for electrochemical detection of H_2O_2 (Song et al., 2013a). This biosensor can rapidly and sensitively detect H_2O_2 down to 0.5 μM. Another electrochemical biosensor was fabricated using graphene modified electrode as support platform for immobilizing cytochrome c (Wang et al., 2012a). This polymer-conjugated graphene nanocomposite exhibited excellent biocompatibility and large specific surface area, contributing to the signals enhancement and the interference reduction. They found that the graphene nanocomposites benefit the electrocatalytic activities for redox reaction and the electrochemical performance for the oxidation of H_2O_2 was also greatly enhanced. Under the optimized condition, it can detect H_2O_2 in the range of 0.5–400 μM sensitively.

Due to its intrinsic properties, graphene nanomaterial has received significant attentions in the construction of diverse sensing platform for cholesterol detection. Gholivand and Khodadadian (2014) developed a selectivity and sensitivity electrochemical cholesterol biosensing platform using graphene-ionic liquid modified cholesterol oxidase as sensing layer. Large specific surface area provided by the graphene layer was introduced to immobilize a branch number of enzyme and a sensitive amperometric response to cholesterol was achieved. This bi-enzymatic cholesterol biosensor presented good reproducibility with low interference from the coexisting compounds in serum. Graphene/PVP/PANI induced current amplification was studied in paper-based cholesterol biosensor, which was designed by electrospraying enzyme-graphene/PVP/PANI layer-by-layer film on the paper based electrodes (Ruecha et al., 2014). This strategy resulted in the current increase up to 3-fold compared to unmodified electrode. The increasing current signal was due to the improvement of dispensability of substrate and the increasing electrochemical conductivity of electrode, leading to low background emission and high sensitivity. In addition, Cao et al. (2013a) adopted an integrated biosensing system to embed cholesterol oxidase in the graphene–Pt–Pd hybrid nanocomposite. The cholesterol oxidase was successively self-assembled to graphene–Pt–Pd hybrid nanocomposite with high load amount and superior biological activity. This fabricated biosensor was further tested with real food sample, indicating the promising performance to serve as facile detection tool in food quality analysis.

Further efforts were aimed at integrating biosensors with real time monitoring and developing advanced electrode nanomaterials. For instance, one example of real-time online continuous glucose and lactate sensing in human serum was described using the flexible printed electrochemical biosensor (Gu et al., 2014). This biosensor was constructed by dual-enzyme working electrode and prepared by modified the electrode surface with graphene hybrid following with the online micro-detection system. This biosensor can simultaneously monitor the glucose and lactate *in vivo* with little cross-talk. With the similar strategy, a real-time graphene based electrochemical biosensor for monitoring of adenosine triphosphate (ATP) was constructed utilizing an ATP aptamer (ATPA) capture probes profound to flavin adenine dinucleotide (FAD) molecules (Sanghavi et al., 2013). The system could quantitatively monitor FAD releasing in real time. Moreover, this device allows various detection units to be built and thereby forming a smart application, which holds great potential for developing a real-time analysis system with little cross-talk and low cost.

3. Graphene-based electrochemical immunosensors

Immunosensors are analytical detection platforms that are based on measuring antibody–antigen specific conjugation reactions (Wang, 2006). Numerous signal generation protocols have been developed based on these antibody–antigen interactions. Immunosensors usually serve as a standard analysis method in biomedical clinical diagnostics in laboratories, in monitoring environmental contamination and in determining food safety (Zhang et al., 2014c; Kang et al., 2013; Li et al., 2010; Zou et al., 2010; Wang et al., 2008). Electrochemical immunosensors have lately been considered an important technology among immunoassays because of their simplicity of use and production, small sample volume, rapid analysis, high sensitivity and good selectivity (Wan et al., 2013). Amperometry, potentiometry and electrochemical impedance spectroscopy (EIS) are the typical electrochemical techniques used in immunosensors. Furthermore, numerous types of point-of-care testing applications based on traditional electrochemical methods have been conducted (Liu et al., 2014a). For

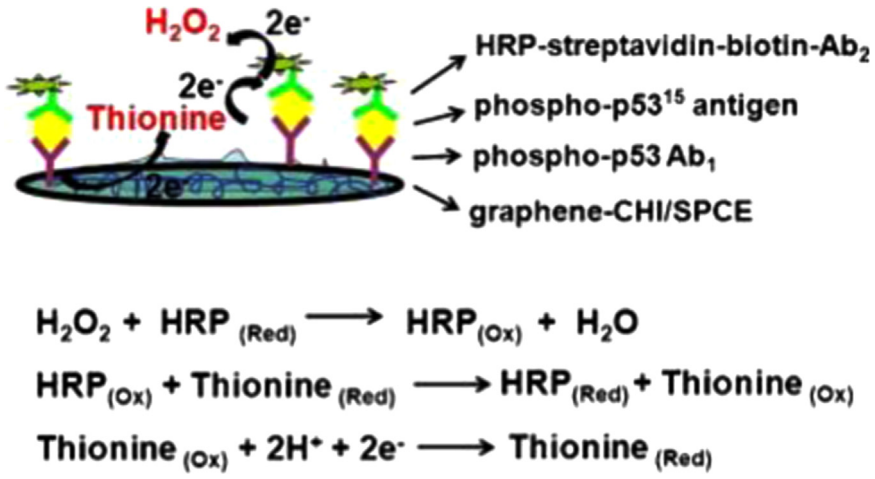

Fig. 5. Schematic illustration of sandwich immunoassay of phosphor-p53. Reproduced from Xie et al. (2011) by permission of Elsevier Science Ltd.

example, paper- or microfluidic-based detection platforms have received considerable attention in immunosensor fabrication (Yetisen et al., 2013; Yan et al., 2012). In recent years, three review articles have summarized the use of electrochemical immunosensors for point-of-care diagnosis (Liu et al., 2014a; Yetisen et al., 2013; Wan et al., 2013).

3.1. Graphene-based electrochemical immunosensors for biomarker detection

The development of reliable, cost-effective, rapid detection for cancer diagnosis is extremely important because of the prevalence of the disease and its potential lethality (Taleat et al., 2014; Vilela et al., 2014; Hasanzadeh et al., 2013). Generally, a biomarker refers to a measurable indicator of a certain biological disorder. Graphene-based electrochemical immunosensors have been developed to detect various low-concentration biomarkers, including carcinoembryonic antigen (CEA), IL-6, human chorionic gonadotropin (hCG), and PSA, which are considered well-known biomarkers due to their unquestionable advantages for the accurate detection of human disorders. For instance, a new sandwich-type immuno-protocol for CEA detection was designed using Ag/Au NPs assembled on graphene as molecular tags. The subsequent current signal for the detection of CEA from the coupled NPs was generated at an *in situ* platform, and promising performance was obtained for the enzyme-free analysis of low-level biomarkers (Huang et al., 2015). A metallic NP/graphene nanostructure with a large specific surface area and high electrical conductivity was synthesized for electrode modification for immunoassays. Specifically, a simple immunoassay with one step construction of graphene/Au hybrid electrode was presented by Zhu et al. (2015b). This immunosensor relied on the hybridization chain reaction (PCR) and biotin combined with Au magnetic NPs to achieve high signal amplification. Benefiting from these factors, it displayed good linear relationships in the ranges from 0.2 to 800 pg mL^{-1} for alpha-fetoprotein (AFP), 0.2 to 600 pg mL^{-1} for CEA, 0.2 to 1000 pg mL^{-1} for CA125 and 0.2 to 800 pg mL^{-1} for PSA with detection limits of 62, 48, 77 and 60 fg mL^{-1}, respectively. In the electrochemical immunosensors, signals are generated via various mechanisms and detected electrochemically. According to the electrochemical detection mechanisms, various important factors need to be addressed to obtain excellent sensitivity in detection. Herein, we just focus on the recent advances in graphene modified biointerfaces, nanomaterials or enzyme-enhanced signal amplification which are very important for the development of graphene based electrochemical immunosensors.

3.1.1. Graphene-based materials as electrode modifiers in development of electrochemical immunosensors

The crucial part of accurate analyte determination is to immobilize the desirable antibody or antigen properly on the solid electrode surface. Graphene, which is characterized by planar covalent-network solids, not only possesses a large specific surface area but also exhibits a unique structure: cavities in the wall surface and tunable morphologies and compositions, which are particularly advantageous for electroanalysis. It has been widely introduced for the immobilization of a series of recognition probes and for the modification of biosensing interfaces with controlled unique structures. Significant contributions have been made to the use of graphene-based 2D materials, which are expected to be employed in the construction of novel sensing platforms. Compared with electrochemical immunosensors that are modified with other nanomaterials, graphene-based electrochemical immunosensors have attracted more attention because of their promising performance in biomedical analysis. As one of the most successful examples, a graphene-based immunosensor was reported to offer well-defined stability and reproducibility in the electrochemical detection of p53 with a wide linear range (Xie et al., 2011). The sandwich immunoassay exhibits good performance for detecting and screening p53 (Fig. 5). The graphene-based sensor platform enhances electron transfer and increases the surface area to carry more captured antibodies simultaneously than other protocols. After this report, several studies successfully extended to graphene based nanomaterials in the exploration of different kinds of electrochemical immunosensors over the past two years. Zhu and Dong (2014) summarized varieties of electrochemical immunosensors using graphene modified electrodes. Wu et al. (2013a) provided an overview of different methods of graphene fabrication with desirable and specific nanostructures along with the technology of electrode modification for electrochemical immunosensors. In the same time, novel fabrication and modification methods have been developed to synthesize various graphene-based nanostructures for developing immunosensors with controlled sizes and shapes. For example, an interleukin-6 electrochemical immunosensor for the detection of interleukin-6 (IL-6) in serum was reported to have a broad detection range and excellent signal-to-noise ratio (Wang et al., 2014a). With appropriate designs, nanocomposites can offer more opportunities for the surface functionalization and the conductivity and electron transfer rate enhancements, and thus improve their electrochemical performances in electrochemical immunosensor. Recently, various hybrid composites comprised of graphene 2D nanomaterials were investigated as novel electrode materials to

construct novel immunosensing platform. For example, a triple signal amplification protocol for the sensitive detection of cancer biomarkers was developed using poly(styrene-co-acrylic acid) microbeads carrying Au NPs as a tracing tag on the graphene-modified electrodes to enhance electron transfer (Lin et al., 2012). The signal was clearly amplified. The excellent analytical performance with high sensitivity, convenient operability, and acceptable reproducibility, stability and accuracy of this novel immunosensor offers great opportunities in clinical application. Using the similar method, a graphene-silica sol–gel modified indium tin oxide (ITO) electrode was employed as the detection platform in this work. It provided a stable nanostructure for the immobilization of primary antibody and exhibited a dynamic working range of 1–40 pg mL^{-1} with a detection limit down to 0.3 pg mL^{-1}. The sensitivity of this immunosensor was fairly similar to the conventional ELISA method and provided a promising ultrasensitive assay for early cancer diagnosis. Moreover, it revealed that the electrical activity of graphene depends significantly on the active edge sites exposed and the surface to volume ratio. Furthermore, a wide variety of complex graphene-based nanomaterials, including magnetic graphene, N-doped graphene, graphene-other carbon material, graphene-noble metal, graphene-transition metal, graphene-metal oxide nanohybrids have been prepared for use as advanced electrode materials for immunosensing applications. Specifically, Lin et al. (2015) developed an electrochemical immunosensor that used a magnetic graphene-modified gold electrode as an analytical platform to determine cancer biomarkers at extremely low concentrations. This immunoassay is reproducible and easily operated. Moreover, it simultaneously implements the detection of rapid vascular endothelial growth factor. A similar strategy was further employed to develop an immunosensor for the direct determination of microRNAs (miRNAs) using a graphene-based platform (Tran et al., 2013). The high sensitivity of this sensor was represented as the capability to distinguish two specific RNA–DNA antibodies for recognizing miRNA–DNA heteroduplexes. The low limit of detection was realized without utilizing any other signal amplification process. The sensitive detection of breast cancer biomarker CA 15-3 was performed using an N-doped graphene-based electrochemical immunosensor (Li et al., 2013a). The detection used a sandwich-structure immunosensor based on highly conductive graphene-modified electrodes. High sensitivity was obtained because N-doped graphene accelerated electron transfer and provided an extremely high active surface area. The choice of hybridization of graphene and metal or other carbon materials also influences the improvement of electrochemical immunosensors significantly. Other group has also investigated graphene/carbon nanomaterials for developing electrochemical immunosensors. Liu et al. (2012b) assembled a uniform CNT/graphene nanocomposite to modify the electrodes for the ultrasensitive detection of human IgG. This layer-by-layer assembled nanocomposite was claimed to promote electron transfer, mass transfer and specific surface area compared with other nanomaterials. Excellent accuracy was achieved for the detection of human IgG in serum samples. Metal oxides generally have poor conductivity, whereas graphene decoration could increase the conductivity and enhance detection signal. Moreover, metal oxides NPs could provide excellent biocompatible surface to be beneficial for immobilization of biomolecules, and thus improve the immunosensor performance. For instance, Yu et al. (2013) fabricated a sensitive label-free immunosensor for kanamycin detection using Ag hybridized mesoporous Fe_3O_4 NPs and graphene to enhance the electrochemical response. Besides metal oxides, noble metals were also exploited to integrate with graphene to develop new electrode materials for electrochemical immunosensors owing to the synergistic contribution among components. Pt NPs combining with graphene was considered to be excellent nanomaterials that was used in a wide variety of biosensing applications due to its high specific surface area and excellent electrocatalytic effects. Singal et al. (2014) employed Pt NPs functionalized graphene nanosheets to develop an immunosensor for human cardiac troponin I. Pt NPs were adsorbed onto the functionalized graphene nanosheets by an electrostatic assembly. The resulted nanocomposite was characterized by good biocompatibility and high Pt NPs loading properties, which can be used to immobilize antibody conjugates (Ab2) to serve as electrochemical probes. This platform provided a high surface area for a uniform distribution of Pt NPs to accommodate more specific antibodies. Moreover, other types of graphene-based nanomaterials were also utilized as advanced electrode materials to design high-performance immunosensors (Wang et al., 2013c; Chen et al., 2013b; Wu et al., 2013b; Lin et al., 2013; Tran et al., 2013; Liu et al., 2012a; Wei et al., 2012; Eissa et al., 2012).

On the other hand, several novel electrochemical label-free immunosensors using graphene-modified electrodes have been reported. For instance, a label-free immunosensor for PSA was proposed using a methylene blue (MB)/graphene-modified electrode (Mao et al., 2012). The inorganic dye, MB, is one superior electrocatalyst for H_2O_2 reduction. It provides broad potential for applying in electrochemical immunosensor owing to their synergistic effect. The electroactive MB was loaded in the inner pores of graphene, which possessed good electrochemical behavior due to their unique surface area and conductivity. Moreover, the electron mediation of MB between electrodes allows high signal amplification. A branched label-free electrochemical immune-platform for the simultaneous detection of two biomarkers was introduced using a similar strategy (Kong et al., 2013). MB and Prussian blue (PB) were selected as redox mediators to indicate different antigens. The essential point is the anti-diffusion of electron mediators on the different electrode surfaces resulting from the increasing spatial blocking and impedance from the formed immune-complex. Liu et al. (2015a) reported a precise and quantitative detection method for CEA using a monolithic and macroporous graphene foam-modified electrode. In this method, a lectin macromolecule monolayer was functionalized on a graphene electrode using *in situ* polymerized PDA.

3.1.2. *Graphene nanosheets as nanocarriers for signal molecules in electrochemical immunosensors*

Given the unique advantages of graphene nanomaterials mentioned above, it is desirable to accommodate highly active probes and targets of interest directly to amplify the electrochemical detection signal. With the unique advantages of graphene nanomaterials in terms of high biocompatibility, electrocatalytic activity, and excellent conductivity, it is desirable to harness their properties in composites through enzyme incorporation for use as an appropriate probe, enhancing the sensitivity of immunosensors. The graphene nanosheet plays a critical role in the construction of an electroactive carrier by enabling effective covalent bonding with active signal probes via π–π stacking interactions. Du et al. (2011) first proposed a new approach for the ultrasensitive detection of p53 based on using enzyme loaded graphene nanosheet as label of reporting antibody of immunoassays. As shown in Fig. 6, excellent sensitivity was achieved because bio-conjugated HRP and p53 antibody were linked to the carboxylate groups of functionalized graphene at extremely high HRP and p53 ratio, whereas the primary antibody was attached to the Au NP-modified screen-printed carbon electrode through the self-assembly procedure. Upon the completion of an enzymatic sandwich immunoreaction, the HRP-p53 Ab2-graphene conjugate was captured on the electrode surface. The graphene carrier could capture considerable signal elements (HRP) via hybridization to facilitate interfacial enzymatic electron

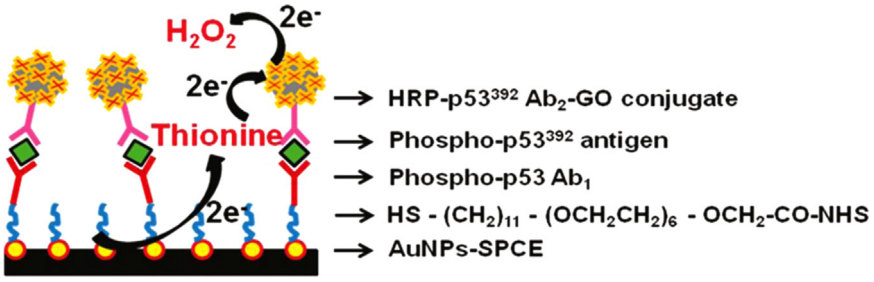

Fig. 6. Schematic Illustration of the multienzyme labeling amplification strategy using HRP-p53 Ab2-Graphene conjugate. Reproduced from Du et al. (2011) by permission of the American Chemical Society.

transfer, which resulted in further signal enhancement. A detection limit down to the picomole range and a broad linear detection range from 0.02 to 2 nM were obtained from this work. Lai et al. (2013) reported the sensitive detection of clenbuterol by loading GOx on functionalized GO nanocomposites. Moreover, multi-nanomaterial-enzyme hybrids combined with graphene composites were used to fabricate a novel biointerface and develop an immunoassay for the sensitive detection of CEA with a detection limit as low as 5 ng mL^{-1} (Jin et al., 2014). This scheme was based on electrochemical enzymatic redox cycling using HRP as an enzyme probe, H_2O_2 as an enzyme substrate, and magnetic beads coated with captured antibodies to avoid reducing the conductivity of graphene. High signal amplification was achieved by enhanced electron transfer between the electrode and the attached enzyme label. Zhang et al. (2014a) developed an enzyme-modified peptide nanowire-labeled immunoassay to detect human substance P (SP) in clinical samples with excellent performance compared with the standard method. Oxidation current amplification was achieved by the large number of HRP molecules attached on the nanowire surface. Because of the heterogeneous nature of the assay, there is no interference by electroactive substances or electrode fouling. Zhu et al. (2013a) integrated three complementary detection strategies for the highly selective and sensitive identification and quantification of three analytes simultaneously using functionalized graphene sheets with redox-probes as tracers. A GO-based electrochemical enzymatic redox-cycling assay was developed for the detection of CA-15-3 (Park et al., 2014). The enzymatic redox cycling combined with simultaneous enzymatic amplification and redox cycling combined with prior enzymatic amplification together provided a high sensitivity with a detection limit of 0.1 U mL^{-1}. A signal amplification protocol for a human IgG immunoassay has been established using the unique properties of GO-based composites (Martín et al., 2015; Haque et al., 2012). This strategy involves poly-layer functional GO sheets conjugated with HRP label captured antibodies through covalent bonding, which are multi-labeled to increase the sensitivity.

Given the unique advantages of graphene nanomaterials, it is desirable to harness their properties in composites through incorporation with various functional nanomaterials. These functional nanomaterials have attracted great interests because of the synergistic contribution of the components. With the synergistic effect, the design of novel nanocomposites that provide higher detection sensitivity compared with enzyme labels has attracted considerable attention for the development of graphene-based immunosensors. Graphene hybrid nanomaterials could yield various exotic properties, depending on their composition, and could offer significant potential in signal amplification (Han et al., 2013). Nobel metals, such as Pt, Pd, and Au, exhibit promising conductivity and outstanding catalytic activity, which benefit for electrochemical biosensing applications. In addition, these nanoscale noble metals could efficiently prevent the aggregation of graphene and enhance the electron transfer by serving as electrical nanowires for shortening electron transfer distance. For example, an enzyme-free ultrasensitive AFP immunosensor was established by combining target-induced hybridization with Pd-graphene nanocomposites (Qi et al., 2014). The strongly catalytic enzyme-like element was immobilized on planar graphene nanosheets to serve as appropriate probes. Additionally, the Pd NPs loaded on graphene nanosheets effectively enhanced the *in situ* catalytic performance and catalytic electron signal transfer rate. The electrochemical signal was amplified remarkably. A broad linear detection range from 0.01 to 12 ng mL^{-1} with a detection limit as low as 5 pg mL^{-1} for AFP was achieved with this approach. Using a similar strategy, Lin et al. (2014) developed a CEA immunoassay using nano-gold induced hybridization of Ag in combination with graphene. Au NP-functionalized carbon foam was employed to couple with Ag NPs as a signal amplification component for the sensitive electrochemical immunosensing of biomarkers. The proposed method achieved a wide linear range from 0.05 pg mL^{-1} to 1 ng mL^{-1} and a detection limit down to 0.024 pg mL^{-1}. A sensitive electrochemical immunosensor based on the self-catalytic growth of Pt NPs on graphene nanosheets as conductive bridges was fabricated to amplify the detection signal of influenza (Yang et al., 2015). Pt-graphene functionalized bioconjugates could be captured through a sandwich-like reaction, and the detection signal was directly amplified from the high local concentration of 1-naphthol, which was produced *in situ* from the hydrolysis of 1-naphthyl phosphate catalyzed by alkaline phosphatase (ALP). Such enzyme-like catalytic activity can enlarge the current signal produced by NPs in solution, resulting in a lower detection limit and holding great promise for biomarker analysis in different applications. In addition, this simplified preparative procedure could be easily achieved because the active signal probes do not require any additional electroactive substrate. A new signal amplification strategy based on ionic liquid doped chitosan matrix and Au NPs-graphene labels has been established with this essential mechanism and has been applied into sensitive detection of cancer biomarker, where the antibody labeled with Au NPs-graphene derivatives probe at the distal end was covalently attached on the matrix surface. A low detection limit, high sensitivity, satisfactory accuracy and selectivity and acceptable stability were achieved. Shen et al. (2014a) constructed a sensitive immunosensor based on dendrimer-functionalized graphene as a label for the detection of α-1-fetoprotein. Based on the high electrocatalytic activity of Pt NPs toward oxygen reduction and methanol oxidation, Xu et al. (2013) developed a novel non-enzymatic Pt NP immunosensor with ultrahigh catalytic efficiency. Moreover, in addition to NPs, outstanding studies of noble metals with different morphologies, such as nanospheres and nanowires, have been carried out. Owing to their unique surface structure and high surface-to-volume ratio, these morphologies have outstanding ability to functionalize graphene in the construction of electrochemical biosensors. Tang et al. (2011) used

biofunctionalized magnetic graphene nanosheets as probes and multifunctional nanogold hollow microspheres (GHS) as distinguishable signal tags for the detection of CEA and AFP in biological fluids. In combination with graphene, several other high-performance immunosensors for the detection of various biomarkers were designed using enzyme-like NPs (Li et al., 2014b; Ge et al., 2014; Feng et al., 2014; Park et al., 2014; Shi et al., 2014; Yang et al., 2013b; Chen et al., 2013b, 2012b; Tan et al., 2013; Cai et al., 2012). Some polymers, such as chitosan and conducting polymers, could be combined with graphene, resulting in the improvement of the sensitivity of analyte detection. Yang et al. (2011a) found that polymer functionalized graphene nanosheets could be efficiently employed for the sensitive detection of cancer biomarkers through labeled amplification. Using the same strategy, Yang et al. (2011b) demonstrated that the ionic liquid-doped chitosan matrix can effectively immobilize antibody due to its good biocompatibility and conductivity. Inspired by pervious researches, considerable efforts have been made to synthesize quantum dot (QD)-graphene nanoconjugates, aiming at amplifying the signal for the detection of cancer biomarkers, such as PSA. The high sensitivity and wide linear range can be ascribed to the increased loading of QDs on the graphene sheet, whereas the enhancement of the transduced detection signal is due to the good conductivity of graphene nanosheets. Using a similar strategy, Shiddiky et al. (2012) reported a sensitive detection method for epithelial cell adhesion molecule using graphene/CdSe QD bionano-conjugates as signal amplifiers. The method enabled detection limits as low as 100 fg mL^{-1} in PBS solution and 1 pg mL^{-1} in serum samples. Wu et al. (2013b) developed an immunosensor based on graphene QD signal amplification for the detection of two disease-specific biomarkers.

3.1.3. Other graphene-based electrochemical immunosensors for biomarker detection

The electrochemical field effect (FET) transistor offers an alternative sensing method to detect various analytes, including ions, protein and biomolecules, which obtained higher sensitivity and better stability compared with traditional electrochemical detection methods. FET offers a promising future because it can be easily designed in accurately quantitative and label-free detection. Some other obvious advantages, such as improved reaction kinetics and less environmental interference to the electrodes have also been reported. He et al. (2012) designed a graphene-based FET to reveal the influence of two important factors (flow velocity and potential drop) for sensitivity. Jang et al. (2015) developed a highly ion-sensitive FET with clear electrical signal enhancement, which enables the development of convenient point-of-care devices. This strategy combined ion-sensitive FET with ELISA to achieve an electrical response generated in the catalytic reaction of the labeled enzyme. High sensitivity was obtained because the orientation of the current and the portability of electroactive species were efficiently controlled by this protocol during the reaction. Highly sensitive analysis of cancer biomarkers in serum was conducted with a graphene-based FET using a similar strategy (Okamoto et al., 2012). Cheng et al. (2014) utilized FET as a promising method to develop a label-free immunosensor for different types of tumor biomarkers, where small receptor antigen binding fragments were immobilized on the graphene-modified platform, offering high sensitivity and a wider concentration range (100 pg mL^{-1} to 1.0 μg mL^{-1}). However, the lack of a band gap in graphene fundamentally limits its sensitivity in FET.

The development of microfluidic or paper-based electrochemical immuno-devices offers great opportunities for rapid detection, separation of interfering agents and effective measurement. Recently, graphene-based microfluidic immunosensors for the detection of biomarkers has become a promising area for point-of-care monitoring and diagnostics. The integration of signal amplification strategy with a microfluidic immunosensor was developed for the multiplexed measurement of cancer biomarkers in serum samples from patients (Wu et al., 2013c). The device was divided into eight individual lines modified by graphene nanomaterials, and each was extremely sensitive to the specific analyte. Silica NPs were used as probes to label the signal antibodies. A positive identification was indicated by the electrochemical current signal and was visually compared with the on-chip reference. Various cancer biomarkers in human samples can be detected due to reaction variability and product stability. Because ambient conditions have tremendous influences on accurate analysis, many attempts have been made to design calibration standards and new amplification protocols without optimal conditions. Wu et al. (2014b) improved their graphene-based microfluidic immune-device by triggering a controlled amplification–by-polymerization on the immune-device surface and achieved a self-calibrating system. This novel signal amplification strategy was claimed to enhance electrochemical signal output significantly to minimize ambient condition impacts and achieve ultrasensitive detection. Another notable study reported that vertically aligned ZnO nanowire arrays were fabricated on a graphene foam-modified electrode in one microfluidic system to selectively detect the biomarkers of Parkinson's disease (Yue et al., 2014). An extremely low detection limit for each analyte was achieved by the modified electrode because of its high surface area and high selectivity. The good stability was explained by the high protective ability for the occupied biomolecules of the graphene foam-modified electrode. These studies demonstrate that graphene materials will greatly accelerate research on developing immunoassays for sensitive detection of biomarkers.

3.2. Graphene-based electrochemical immunosensors for pathogen detection

Recently, foodborne pathogenic bacteria have become a major public health concern. Rapid and easily performed detection of various families of foodborne pathogenic bacteria, such as *Escherichia coli* O157: H7, has become necessary. Therefore, graphene-based electrochemical immunoassays have attracted considerable attention and have been intensively studied to achieve such detection. Various strategies have been pursued to develop nanomaterial-based signal enhancement, benefiting the fabrication of novel electrochemical immunosensors. For example, label-free electrochemical immunosensors have been considered as a promising candidate strategy for the detection of pathogens, such as the similar protocol in electrochemical immunosensors for biomarker detection. A label-free electrochemical detection method for *E. coli* O157:H7 using Au NP modified free standing graphene paper as novel affinity agents achieved important architectural improvements by using captured antibodies and high sensitivity for the detection of *E. coli*. It provided new insight into the design of flexible immunosensors (Wang et al., 2013c). Qi et al. (2013) introduced a bio-imprinting technique for label-free ultrasensitive and quantitative detection of sulfate-reducing bacteria (SRB) in the range of 10^4–10^8 CFU mL^{-1} with a similar protocol. Briefly, multilayer reduced-graphene nanosheets were electrodeposited along with chitosan on the surface of ITO, followed by the absorption of SRB and a thin coating layer of chitosan around the bacteria. This approach can also distinguish other control strains based on the size and shape differences from other bioreceptor combinations.

Multiplexed graphene-based electrochemical immunoassays incorporating different signal amplification strategies can offer selective and sensitive platforms for measuring various pathogens simultaneously. Wang et al. (2012b) integrated a dual signal amplification detection strategy for the identification and

Table 2
Graphene-based immunosensors.

Analyte	Graphene modified electrode	Detection range	Reference
CEA	PdCu/graphene nanosheet	0.01–12 ng mL^{-1}	Cai et al. (2012)
	PB/graphene nanosheet	0.5–60 ng mL^{-1}	Chen et al. (2013b)
	Thionine/graphene	0.6–80 ng mL^{-1}	Feng et al. (2014)
	Au NPs/graphene/thionine	0.1–1 × 10^9 fg mL^{-1}	Han et al. (2013)
	Ag/Au NPs/graphene	10–1.2 × 10^5 pg mL^{-1}	Huang et al. (2015)
	Au/MB/graphene	5–60 ng mL^{-1}	Jin et al. (2014)
	MB/graphene nanosheet	0.5–80 ng mL^{-1}	Kong et al. (2013)
	Au/MCF/graphene	0.05–1000 pg mL^{-1}	Lin et al. (2014)
	Graphene foam	0.1–750 ng mL^{-1}	Liu et al. (2015a)
	Graphene nanosheet/Au	0.01–200 ng mL^{-1}	Tang et al. (2011)
	HRP/graphene/polymer	0.01 ng mL^{-1}	Wu et al. (2014b)
	Au/Nafion/graphene sheet	0.01–50 ng mL^{-1}	Zhu et al. (2013a)
	Au/graphene/HCR	0.2–600 pg mL^{-1}	Zhu et al. (2015b)
AFP	Graphene/FET	0.0001–1 μg mL^{-1}	Cheng et al. (2014)
	Graphene/SWCNT	0.1–100 ng mL^{-1}	Lin et al. (2013)
	Pd/graphene	0.01–12 ng mL^{-1}	Qi et al. (2014)
	HRP/graphene	1–100 ng mL^{-1}	Shen et al. (2014a)
	HRP/graphene/polymer	0.01 ng mL^{-1}	Wu et al. (2014b)
	Au/Nafion/graphene sheet	0.016–50 ng mL^{-1}	Zhu et al. (2013a)
	Au/graphene/HCR	0.2–800 pg mL^{-1}	Zhu et al. (2015b)
p53	HRP/functional graphene	0.02–2 nM	Du et al. (2011)
	HRP/graphene	0.2–10 ng mL^{-1}	Xie et al. (2011)
β-lactoglobulin	Organic film/graphene	0.001–100 ng mL^{-1}	Eissa et al. (2012)
CA-153	Silica NPs/graphene	0.001–200 U mL^{-1}	Ge et al. (2014)
	N-doped graphene	0.1–20 U mL^{-1}	Li et al. (2013a)
	PtFe alloy/graphene	0.002–40 U mL^{-1}	Li et al. (2014b)
	Graphene/ITO	0.1–10 pg mL^{-1}	Park et al. (2014)
	HRP/graphene/polymer	0.05 ng mL^{-1}	Wu et al. (2014b)
E. coli O157:H7	Au NPs/graphene/PEDOT	7.8 × 10–7.8 × 10^6 CFU mL^{-1}	Guo et al. (2015)
	PolyG/graphene	1 pM	Wang et al. (2012b)
	Au NPs/graphene	1.5 × 10^2–1.5 × 10^7 CFU mL^{-1}	Wang et al. (2013c)
SRB	Graphene/chitosan	1 × 10^4–1 × 10^8 CFU mL^{-1}	Qi et al. (2013)
IgG	Poly(BMA)/R-graphene	700 fg mL^{-1}	Haque et al. (2012)
	PANI/graphene	9.7 pg mL^{-1}	Lai et al. (2014)
	Reduced graphene	1–500 ng mL^{-1}	Liu et al. (2012b)
	Fc/Au/graphene	1–300 ng mL^{-1}	Wang et al. (2013a)
	PtNDs/graphene	0.001–10 ng mL^{-1}	Xu et al. (2013)
	Au NPs/graphene/ion liquid	0.2–500 ng mL^{-1}	Yang et al. (2011b)
Troponin 1	Pt/graphene	0.01–10 ng mL^{-1}	Singal et al. (2014)
IL-5	Ion/ALP/graphene	0.001–10 ng mL^{-1}	Jang et al. (2015)
IL-6	Au/Si/graphene sol–gel	1–40 pg mL^{-1}	Wang et al. (2014a)
MMP-9	PDA/GNR	10^{-5}–10^3 ng mL^{-1}	Shi et al. (2014)
MMP-2	Au NPs/N doped graphene	0.0005–50 ng mL^{-1}	Yang et al. (2013b)
MCU1	MB/poly ABA/graphene	1–12 ppb	Taleat et al. (2014)
IgM	Au/Fe_3O_4/graphene	0.0375–18 AU mL^{-1}	Jiang et al. (2013)
Clenbuterol	PB/functional graphene	0.5–1000 ng mL^{-1}	Lai et al. (2013)
PSA	Fe_3O_4/graphene	0.01–40 ng mL^{-1}	Li et al. (2011)
	Au/poly microbead/graphene	0.0005–0.5 ng mL^{-1}	Lin et al. (2012)
	Graphene/MB/chitosan	0.05–5 ng mL^{-1}	Mao et al. (2012)
	QDs/graphene sheet	0.005–10 ng mL^{-1}	Yang et al. (2011a)
	Au/graphene/HCR	0.2–800 pg mL^{-1}	Zhu et al. (2015b)
Vascular endothelial growth factor	Au/Magnetic graphene	31.25–2000 pg mL^{-1}	Lin et al. (2015)
HSP	Graphene/FET	2.3 nM	Okamoto et al. (2012)
EpCAM	CdSe QDs/graphene	1–500 fg mL^{-1}	Shiddiky et al. (2012)
	QDs/Si/graphene		Wu et al. (2013b)
Ache	QDs/graphene	0.3–300 ng mL^{-1}	Wang et al. (2008)
Kanamycin	Graphene/Nafion/thionine/Pt	0.01–12 ng mL^{-1}	Wei et al. (2012)
	Ag/Fe_3O_4/graphene sheet	0.05–16 ng mL^{-1}	Yu et al. (2013)
Shewanella	Ag NPs/graphene/Au NPs	7 − 7 × 10^7 CFU mL^{-1}	Wen et al. (2014)
Cysteine	GNR/Nafion	0.025–500 μM	Wu et al. (2012)
Influenza	Pt/CeO_2/graphene	0.001–1 ng mL^{-1}	Yang et al. (2015)
Parkinson's disease	ZnO/graphene foam	1 nM	Yue et al. (2014)
Substance P (SP)	Fc/Au NPs/graphene	0.015 ng mL^{-1}	Zhang et al. (2014a)
APE1	Au NPs/graphene	0.1–80 pg mL^{-1}	Zhong et al. (2014)
PDGF	Graphene/SWCNT	0.02–45 nM	Bai et al. (2012)

quantification of pathogenic bacteria based on bio-barcode labels as a natural bio-receptor with a low detection limit at the pico-molar level. These amplification and viability assays employed a bio-barcode as a recognition probe in a label-free electrochemical immunosensor. Guo et al. (2015) successfully developed a multi-plexed immunoassay for the detection of *E. coli* O157:H7 using a sulfonated graphene (SG)-poly-(3,4-ethylenedioxythiophene) (PEDOT)-Au nanocomposite-modified electrode with a corrected linear response from 10 to 10^6 CFU mL^{-1} and saturation at 3.4 × 10 CFU mL^{-1} under optimal conditions. They fabricated an immunoassay array by the immobilization of HRP-anti-*E. coli* onto the electrode surface to form a sandwich-like system via specific

identification. In another work, an Ag NP-enhanced strategy has been optimized to enable the specific detection of the pathogenic bacteria *Shewanella oneidensis* in human saliva, showing a linear response from 7 to 7×10^7 CFU mL^{-1} (Wen et al., 2014). Graphene was used as a base layer for the conjugation of antibodies. The conjugates binding on the target produced an enhanced immune-recognition response by the reduction of silver ion in the presence of hydroquinone.

3.3. Other interests

Multiplexed graphene based electrochemical immunosensors have been investigated and fully reviewed for other clinical or point-of-care use recently (Li et al., 2014a; Zhong et al., 2014), such as multiplexed NPs based electrochemical immunosensors (Yang et al., 2013f) and multiplexed protein detection and translation of cancer diagnostics (Rusling, 2013).

An ultrasensitive graphene based HRP-PANI immunoassay for quantitative analysis of human IgG was investigated to achieve wide linear detection range and high detection sensitivity with completely excluded conventional interference from dissolved oxygen (Lai et al., 2014). Graphene modified electrode surface was employed to enhance electron transfer, resulting in signal amplification. HRP modified gold NPs was utilized as tracing tag to label on the capture antibodies. Wang et al. (2013a) designed one low-cost, rapid and highly stabile immunoassay that realizes simultaneous detection of different biological analyses. Graphene modified electrodes were utilized to provide large surface area and to accelerate electron transfer at electrode surface. High sensitivity with low concentration sample was obtained because this graphene based immunosensor chose ferrocene (Fc) derivatives as the label. This work offers great potential on sensitive and selective detections of several biological targets, including tumor biomarkers and human IgG. Bai et al. (2012) proposed a sandwich-like graphene based electrochemical biosensor for simultaneously sensitive detection of multiple analytes based on dual signal amplifiers. Namely, single-wall carbon nanotubes (SWCNT) and graphene nanosheets were chosen as two different carriers for redox probes. This biosensor was fabricated via bienzyme modified redox probes-graphene nanocomposites as the tracer label for secondary aptamers through sandwiched assay. The biosensor can simultaneously respond to multiple targets in the sample by integrated with different redox active substrates. Liu et al. (2012b) reported one easy protocol for IgG immunoassay using layer-by-layer assembly of graphene and CNT. Monoclonal anti-IgG antibodies were conjugated onto graphene-CNT assembled interface. The excellent selectivity and low signal to noise ratio is attributed to accelerated electron transfer, mass transfer, and increased specific surface area. Organic–inorganic-poly-thionine-Au–Fe_3O_4 NPs with heterostructure's were synthesized to label an advanced multiplexed graphene-based immunosensor to enhance the reduction ability toward H_2O_2. The sensitivity was greatly improved due to the good conductivity and biocompatibility of the integrated Au–Fe_3O_4 NPs and graphene sheet (Jiang et al., 2013).

Considerable attempts have been made to develop and improve graphene based electrochemical immunosensors. Low cost, rapid and accurate detection of various analytes has been achieved recently. Besides these achievements, the simultaneous detection of multiple targets in complex samples still remains unsolved; and the integration of graphene based electrochemical immunoassay into different analytical devices remains to be eye-caught in clinical point-of-care analysis (Table 2).

4. Graphene-based electrochemical genosensors

Genosensors have advanced greatly over the past three years with better performance and higher sensitivity. Among the numerous nucleic acid assay methods, electrochemical DNA sensors hold promising potential for DNA analysis and sequencing (Zhao et al., 2014; Liu et al., 2012c). Graphene and graphene-based nanocomposites exhibit several advantages and exceed other electrode materials in the catalytic oxidation of the four DNA bases by their exposed edge-like planes (Vashist and Luong, 2015; Wang et al., 2013b). Significant contributions have been made to the synthesis of various graphene-like nanomaterials, which are expected to be employed in the construction of novel sensing platforms for the sensitive and selective detection of DNA bases, nucleotides, single-stranded DNA (ssDNA), and double-stranded DNA (dsDNA) (Gao et al., 2014a; Chen et al., 2012a; Akhavan et al., 2012).

The large specific surface area of graphene nanomaterials could provide an excellent platform for immobilizing related DNA base rings via π–π stacking interactions. The main principle of electrochemical DNA biosensors is based on specific hybridization between the probe DNA and the target DNA. The ssDNA, which is used as the probe DNA, is immobilized onto the electrode surface by covalent interaction or physical adsorption to hybridize to the complementary target DNAs. The post-hybridization electrochemical signal will be monitored by an electrochemical workstation for the change in the conductivity and interfacial property of the electrode caused by the hybridization.

4.1. Graphene-based electrochemical genosensors for nucleic acid assay

4.1.1. Graphene-based electrochemical genosensors for DNA detection

Label-free biosensors have aroused significant attention for the construction of diverse electrochemical DNA sensing platforms due to their simplicity and sensitivity. To overcome the limitation of label-free technique, various electroactive materials can be introduced to functionalize the graphene modified onto the electrodes. Guo et al. (2013b) took advantage of the electroactive dye Azophloxine (AP), a negatively charged water-soluble dye with a large planar aromatic surface, to construct a novel ultrasensitive electrochemical DNA biosensor. The attachment of AP on the graphene surface prevented the agglomeration of graphene while endowing the graphene with excellent electroactive properties. This label-free sensor has achieved a detection limit as low as 4.0×10^{-16} M and has provided great potential for investigating single nucleotide polymorphisms (SNPs). Besides, Signal indicators such as thionine and MB are usually used to functionalize graphene to produce a high response signal (Chen et al., 2013a; Zhu et al., 2012).

Electrochemical impedance spectroscopy (EIS), a newly emerged high-sensitivity analysis, has attracted substantial research interest because it not only provides label-free detection of gene sequences but also exhibits high sensitivity with low background. EIS allows analyses of both resistive and capacitive properties for electrode attachment, such as DNA and RNA. Hu et al. (2012a) demonstrated a simple and label-free electrochemical assay for DNA hybridization using undecorated GO as the sensing platform. The adsorbed ssDNA consists of an immobilization sequence and a probe sequence, and only the probe sequence captures the target ssDNA to form double helical DNA in the presence of the target. EIS was chosen to monitor the interfacial property changes. Sun et al. (2012b) designed an electrochemical DNA biosensor based on a carboxyl-functionalized GO for the detection of gene sequences related to vibrio parahaemolyticus. Poly-L-lysine was used to modify the electrode to form a poly amino acid film which exhibits good stability and reproducibility due to the presence of multiple functional groups. To avoid unwanted defects to

graphene and preserve its integrity and the electronic structure various aromatic organic molecules have been conjugated to the graphene sheet via π-stacking interaction. Hu et al. (2012b) decorated graphene with positively charged N, N-bis-(1-aminopropyl-3- propylimidazol salt)-3,4,9,10-perylene tetracarboxylic acid diimide (PDI). The PDI facilitates ssDNA immobilization by the electrostatic interaction between its imidazole rings and the phosphate backbone of ssDNA, leaving the DNA bases available for efficient hybridization. Zhang et al. (2014a, 2104b, 2140c, 2014d, 2014e) and Luo et al. (2013) fabricated 1-aminopyrene-graphene and tryptamine-graphene hybrids by π-stacking to construct DNA sensors with high sensitivity and selectivity.

Benvidi et al. (2014) designed a novel label-free biosensor for the sensitive detection of specific ssDNA Amelogenin (AMEL) gene, a marker of sex determination, using a reduced graphene oxide (RGO)-modified GCE. As ssDNA is adsorbed on graphene mainly due to non-covalent interaction between the rings in DNA bases and the hexagonal cells of graphene, the adsorption may be disturbed after hybridization.

Signal amplification is another necessary element to enhance the sensitivity of biosensors and to enable gene analysis in real samples. Despite of the unique advantages of graphene, it is desirable to manipulate their properties via coupling with various functional materials to perform a synergistic contribution to signal amplification (Zhu et al., 2015a; Wu et al., 2014a). Recently, various hybrid graphene nanocomposites have been prepared and employed as electrocatalysts in genosensors. For example, Au NPs with different morphology have been designed in DNA-based electrochemical sensors. Sun et al. (2012a) presented an electrochemical DNA biosensor for a *Listeria monocytogenes* assay using an electrochemically reduced graphene/Au NP nanocomposite-modified carbon ionic liquid electrode (CILE) as the platform. Govindhan et al. (2015) synthesized an Au NP/RGO nanocomposite to fabricate a sensing platform for a NADH assay through the *in situ* electrochemical reduction of GO and Au^{3+} with a 100% usage of the precursors. The prepared sensor was further utilized to detect NADH in human urine samples. Rasheed and Sandhyarani (2014) fabricated an easy DNA biosensor for the ultrasensitive detection of the BRCA1 gene using a "sandwich" detection strategy in which the capture probe (DNA-c) and Au NP-linked reporter probe (DNA-r) DNAs hybridized to the target probe DNA (DNA-t). The oxidation of Au NPs was monitored by cyclic voltammetry and chronoamperometry, and a detection limit of 1 fM was achieved, which is lower than reported for other types. In another work, poly(amidoamine) dendrimer (PAMAM) with graphene core (GG1PAMAM) was synthesized and was immobilized on the Au transducer surface (Zhang et al., 2015a, 2015b; Jayakumar et al., 2012). Au nanoparticles then decorated the GG1PAMAM and used for electrochemical DNA hybridization sensing. Furthermore, Au NPs electrodeposited onto the electrodes not only increase electrical conductivity but also improve the electrochemical response in biosensing (Wang et al., 2012c). Similarly, Huang et al. (2014) also constructed a DNA biosensor based on Ag NPs/polydopamine@graphene nanocomposite film for ssDNA assay.

Conducting polymer nanomaterials are also exploited as excellent candidates for electrode materials to fabricate electrochemical DNA biosensors because of their unique and controllable chemical and electrical properties (Yoon and Jang, 2009). To simplify the operation of constructing a biosensor, one-step electrochemical synthesis of the reduced graphene oxide (RGO) has been reported. Jiao's group has proposed several electrosynthesis methods for fabricating polymer- and RGO-based biosensors. They proposed a one-step synchronous electrosynthesis of poly(xanthurenic acid)-RGO nanocomposite, which promotes the electron transfer ability of the electrode and furnishes a synergistic effect between RGO and poly(xanthurenic acid). The resultant sensing platform could sensitively recognize its target DNA using the classical indicator of $[Fe(CN)_6]^{3-/4-}$ and achieved a detection limit as low as 4.2×10^{-15} mol/L (Yang et al., 2013b). Subsequently, they further presented the direct and freely switchable detection of target genes through the one-step electrochemical synthesis of RGO/poly(m-aminobenzenesulfonic acid) (PABSA) nanocomposites via the pulse potentiostatic method. Moreover, the electrochemical reduction of RGO was performed during the resting period of the electropolymerization of PABSA (Yang et al., 2013c). In another study, they utilized the self-redox signal of sulfonated PANI, significantly enhanced by GO, for direct DNA impedance detection. The self-redox signal of the resulting nanocomposite was attributed to the abundant sulfonic acid groups of sulfonated PANI. Compared with the outer classic impedance probe $[Fe(CN)_6]^{3-/4-}$, the inner impedance value of sulfonated polyaniline (SPANI) increased remarkably (Yang et al., 2013a). To evaluate the effect of morphology of the sensor substrate on DNA detection sensitivity, Yang et al. (2014) prepared graphene-based PANI nanocomposites with different morphologies as a model to compare their DNA sensing behaviors. According to the results of their research, vertical arrays exhibited the highest sensitivity by about two orders of magnitude.

Among a variety of DNA signal transducers, DNA sandwich assays have expanded from fluorescence assays to electrochemical assays (Shen et al., 2014b). The detectable electrochemical signals are produced by the signal probes modified with electrochemical or redox labels when the target binding brings them proximal to the electrode. However, a redox label can only transfer minority electrons to or from the electrode surface, which hinders the sensitivity of a DNA sandwich assay. To address this issue, enzyme-based signal amplification for DNA sandwich assays has been extensively explored. Enzymes such as HRP, ALP and GOx are well-known substitutes for the redox label and provide steady recognition and signal amplification. Using HRP/carbon spheres (CNS) as tracers, Dong et al. (2012a, 2012b) designed an ultrasensitive electrochemical DNA biosensor based on an electrochemically reduced GO/Au NP-modified electrode. They found that this hetero-nanostructure improved the conductivity, and the signal was significantly amplified due to the compositional synergy. Contrary to Dong's work, Wang et al. (2013a, 2013b, 2013c) developed a DNA sensor based on Au NPs-single-walled carbon nanohorn (SWCNH) composite modified glassy carbon electrode. Carboxylic GO was chosen as a carrier to load the porphyrin-based mimic as well as trace label for biosensing, which showed greatly enhanced peroxidase activity toward o-phenylenediamine (o-PD) oxidization in the presence of H_2O_2, leading to improved sensitivity for electrochemical biosensing. Recently, Esteban-Fernández de Ávila et al. (2015) designed a disposable electrochemical DNA sensor based on carbonxymethylcellulose-RGO modified screen-printed carbon electrodes. HRP was used to catalyze the redox mediator, tetramethylbenzidine (TMB), and the substrate, H_2O_2, for the detection of the p53 tumor suppressor gene.

In addition to the contribution of HRP in the enzyme-based sandwich assay, ALP was another candidate for the sandwich assay. Wang et al. (2014a, 2014b, 2014c, 2014d) modified the GCE through layer-by-layer assembly of graphene-chitosa-polyaniline to propose a biosensor for the detection of BCR/ABL fusion gene from real samples.

Peptide nucleic acid (PNA) is an analog of DNA and was first used as a fluorescent probe to detect target DNA or RNA in a GO-based assay method by Zhang's group (Guo et al., 2013a; Park et al., 2013). Because of its neutral character, suitable distance between the nucleobases, rigid amido bonds, highly flexible aminoethyl linkers, and intramolecular hydrogen bonding, PNA has been further developed into a PNA-functionalized Si NW-RGO FET biosensor for DNA detection (Cai et al., 2014). The RGO FET

biosensor was able to distinguish complementary DNA from one-base mismatched DNA and non-complementary DNA. This sensor received significant interest because of its high quenching efficiencies and ultrasensitivity, with detection limit as low as 100 fM, which is one order of magnitude lower than previously reported values. In another article, Zhang's group investigated a highly sensitive and selective strategy for DNA detection using electrochemically reduced GO as nanocarriers and PNA as a signal amplification protocol (Du et al., 2013).

Solid-state nanopores have emerged as single-molecule sensors and could potentially be used to rapidly sequence DNA molecules. Graphene has overcome the challenge for fabricating the nanopores in insulating membranes as thick as 15 bases which typically made it difficult for the devices to read individual bases, at 0.335 nm thick. Traversi et al. (2013) demonstrated a nanoribbon transistor to create a sensor for DNA translocation. Simultaneously, Schneider et al. (2013) demonstrated a novel scheme to prevent DNA-graphene interactions by blocking the strong nonspecific hydrophobic interactions between DNA and graphene based on a tailored self-assembled monolayer. They found that ssDNA was detected in graphene nanopores with excellent nanopores durability and reproducibility. Freedman et al. (2013) detected long and short DNA using nanopores with graphitic polyhedral edges and found that the ssDNA translocated much more slowly, allowing the detection of extremely short fragments. Puster et al. (2013) fabricated a GNR nanopores sensor for DNA detection to avoid electron beam-induced damage.

4.1.2. Graphene-based electrochemical genosensors for miRNA detection

Using an enzyme-based nucleic acid sandwich assays, Yin et al. (2012) developed an ultrasensitive electrochemical platform for miRNA detection based on graphene/Au NP-modified GCE for locked nucleic acid (LNA)-integrated MB probes and multifunctionally encoded DNA-Au NPs-LNA bio bar codes coupled with HRP for signal amplification (Fig. 7). The 5′-end of the MB was complementary to the target miRNA, whereas its 3′-end was complementary to LNA-integrated DNA in DNA-AuNPs-LNA bio bar codes. To improve the sensitivity of polymer/graphene sensors and decrease the background signal, Tran et al. (2013) reported a conducting polymer/RGO-based electrochemical biosensor to detect two different miRNAs. Cross-hybridization experiments illustrated that a significant current increase occurred only in the presence of complementary target DNA. In addition to the miRNA assay through classical hybridization, an original approach based on the specific recognition of antibodies and DNA–RNA hybrids with steric hindrance led to a decrease in current.

4.1.3. Graphene-based electrochemical genosensors for adenosine detection

Gao et al. (2014b) developed a sensitive electrochemical biosensor for the detection of adenine and guanine based on porous structure films of over-oxidized polypyrrole/graphene (PPyox/GR). The permselective polymer coatings play a significant role in decreasing background current and increasing the electroactive surface area of graphene. This sensor exhibited a linear working range of 0.06–100 mM and 0.04–100 mM and a low detection limit of 0.02 μM and 0.01 μM for adenine and guanine, respectively. Unlike assays based on capture probe-immobilized electrodes, Sanghavi et al. (2013) presented a double-surface competitive assay that was free of wash steps and enabled the real-time quantitative monitoring of ATP over a five-log concentration range. This recognition strategy was based on an ATPA capture probe that bound to electroactive FAD with a weaker affinity and utilized graphene and Au NPs to enhance electron transfer and sensitivity. The current signal response can be monitored based on the release of FAD. This real-time monitoring method can be extremely useful for the detection of miRNAs expressed in different cancer types.

4.2. Graphene-based electrochemical genosensors for metal ions detection

Metal ions, including Cu^{2+}, Hg^{2+}, Ag^{+} and K^{+}, are important to human health and the detection of metal ions in biological

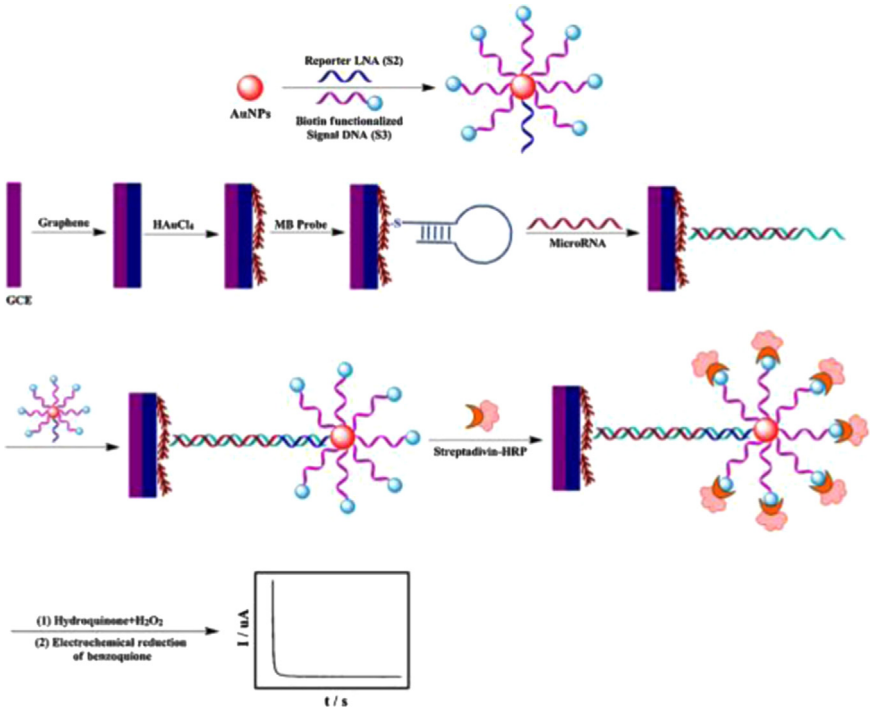

Fig. 7. Chronoamperometry determination of miRNA hybridization through three steps of amplification. Reproduced from Yin et al. (2012) by permission of Elsevier Science Ltd.

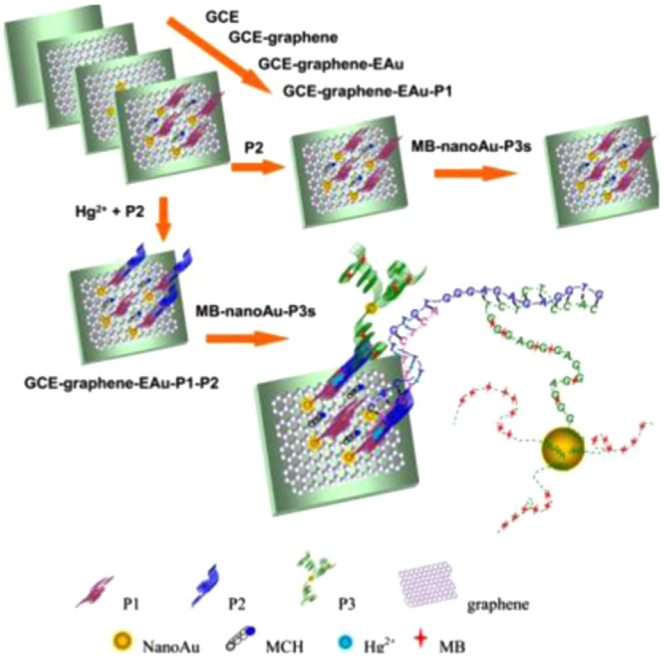

Fig. 8. Sketch map of the sensing strategy for mercury detection. Reproduced from Zhang et al. (2015a, 2015b) by permission of the American Chemical Society.

systems are very important (Gao et al., 2014a). Zhang et al. (2015a, 2015b) constructed a biosensor which Au NPs was electrodeposited onto the electrodes to modify the electrode coupled with graphene. Three ssDNA probes were immobilized onto the electrode, namely a 10-mer thymine-rich DNA probe, a 29-mer guanine-rich DNA probe and a 22-mer thymine-rich DNA probe, for attomolar Hg^{2+} detection (Fig. 8). Tang et al. (2014) reported a label-free electrochemical sensor for Hg^{2+} detection based on the specific T–Hg^{2+}–T cooperation and $HAuCl_4/NH_2OH$ reaction.

4.3. Graphene-based electrochemical detection of DNA damage

DNA damage may be caused by interactions with chemical or physical agents from the environment or normal metabolic processes inside the cell. DNA mutation and tumor generation occur if the damage cannot be repaired in a timely manner. Various types of sensors have been developed for the identification and quantification of DNA damage products. Zhou et al. (2012a, 2012b) reported a hairpin molecular beacon tagged with carboxyfluorescein in combination with GO as a quencher reagent to detect DNA damage by chemical reagents. Four compounds, chlorpyrifos-methyl (CM), mandelieaeids (MA), phenylglyoxylieaeids (PGA) and epoxystyrene (SO), were studied as models to evaluate the damaging effect. The base 8-hydroxy-2′-deoxyguanosine (8-OH-dG) is the most abundant oxidative product of DNA and is also considered to be a biomarker of oxidative DNA damage. Jia et al. (2015) prepared a ssDNA electrochemical biosensor based on functionalized graphene nanosheets for the detection of 8-OH-dG. The biosensor was further utilized to detect 8-OH-dG in real urine and serum samples by using uricase to eliminate interference from uric acid.

4.4. Other interests

Pt NPs (Xie et al., 2012), magnetic NPs (Tiwari et al., 2015; Teymourian et al., 2013) were incorporated with graphene for fabrication of electrochemical biosensors. Sometimes, multiply nanomaterials were integrated for a highly sensitive biosensor. Xie et al. (2012) proposed a complex graphene/Pd NPs/Au/hemin/G-quadruplex-based biointerface, which was also rationally designed to fabricate aptamer sensors, achieving the sensitive detection of thrombin. Yuan et al. (2013) fabricated a dendrimer

Table 3
Graphene-based electrochemical genosensors.

Analyst	Graphene modified electrode	Detection range (LOD)	Reference
ssDNA	GCE/PLLy/Graphene/ssDNA probe	1×10^{-6}–1 μM (16.9 pM)	Sun et al. (2012b)
	GCE/Graphene/ssDNA probe	1×10^{-6}–1 μM (11 pM)	Hu et al. (2012a)
	GCE/ERGO/PNA probe	1×10^{-6}–10 μM (54.6 pM)	Du et al. (2013)
	GCE/Graphene/AP/ssDNA probe	1×10^{-3}–10 pM (0.4 fM)	Guo et al. (2013b)
	SiNW /RGO/PNA probe	(100 fM)	Cai et al. (2014)
	GCE/PXa-ERGO/ssDNA probe	1×10^{-7}–100 μM (4.2 fM)	Yang et al. (2013d)
	Au/Graphene/Au NPs/ssDAN probe	0.025–1.25 nM (8.33 pM)	Niu et al. (2013)
	GCE/ERGO/Au-ssDNA probe	1×10^{-5}–0.1 pM (5 aM)	Dong et al. (2012b)
	GCE/GO/AuNPs-ssDNA probe	(100 fM)	Wang et al. (2012c)
	Au/PAMAM/Graphene/Au/ssDNA probe	1×10^{-9}–1 mM (1 pM)	Jayakumar et al. (2012)
	GCE/Graphene/Pdop/AgNPs-ssDNA probe	1×10^{-9}–100 mM (3.2 fM)	Huang et al. (2014)
	GCE/Graphene/thionine/ ssDNA probe	1×10^{-9}–0.1 mM (0.126 pM)	Zhou et al. (2012a)
	GCE/Graphene/TRA/ssDNA probe	1×10^{-9}–0.1 mM (0.52 pM)	Zhang et al. (2014e)
	GCE/Graphene/PDI/ssDNA probe	1×10^{-6}–1 μM (0.55 pM)	Hu et al. (2012b)
	GCE/Graphene/1-aminopyrene/ssDNA probe	0.01–10 nM (0.45 pM)	Wang et al. (2013b)
Damaged DNA	GCE/Graphene/MB-FAM	–	Zhou et al. (2012a)
BRCA1 gene	GCE/Graphene/ssDNA probe	(1 fM)	Rasheed and Sandhyarani (2014)
AMEL gene	GCE/RGO/ssDNA probe	1×10^{-5}–10 fM (0.0032 aM)	Benvidi et al. (2014)
hly gene	CILE/Graphene/Au NPs/ssDNA	1×10^{-6}–1 μM (0.29 pM)	Sun et al. (2012a)
BCR/ABL fusion gene	GCE/GS-CS/PANI/Au NPs/hairpin DNA probe	0.01–1 nM (2.11 pM)	Wang et al. (2014b)
PML/RARA fusion gene	CPE/GO/SPAN/ssDNA	1×10^{-10}–0.1 mM (0.032 pM)	Yang et al. (2013e)
AdenineGuanine	GCE/PPyox/Graphene	0.06–100 mM (0.02 μM)	Gao et al. (2014b)
		0.04–100 mM (0.01 μM)	
ATP	GPE/Graphene/Au NPs/ATPA/FAD	0.0114–30 μM (201 nM)	Sanghavi et al. (2013)
miRNA	GPE/Graphene/Den Au/MB probe	(0.06 pM)	Yin et al. (2012)
NADH	GCE/RGO/Au NPs	0.05–500 μM (1.13 nM)	Govindhan et al. (2015)
8-OH-dG	GCE/Graphene/ssDNA probe	(0.875 nM)	Jia et al. (2015)
Hg^{2+}	GCE/RGO-CS/T-rich DNA probe	(0.06 nM)	Tang et al. (2014)
	GCE/Graphene/AuNPs/P1,P2,P3 DNA probe	1×10^{-9}–100 nM (0.001 aM)	Zhang et al. (2015b)
Thrombin	GCE/AuNPs/TBAI	1×10^{-4}–50 nM (0.03 pM)	Xie et al. (2012)
Glucose	GCE/Graphene	0.005–20 mM	Zhu et al. (2013b)

polyamidoamine-functionalized RGO with a hemin/G-quadruplex to construct a robust biointerface, which yielded a dual signal amplified electrochemical DNA biosensor to detect thrombin. In another work, a graphene/Au NPs/PANI/GOx nanocomplex-based biointerface was rationally designed to fabricate an aptasensor and achieved sensitive detection of thrombin (Bai et al., 2013a). Moreover, Zhu et al. (2013a, 2013b) combined three cascade chemical reactions with graphene-DNA interaction to develop a new strategy for biosensor fabrication. Glucose was adopted as a model to trigger the cascade chemical reactions, followed by the exposure of palindrome DNA cleaved into pieces to interact with graphene (Table 3).

5. Conclusion

The favorable structural and compositional synergy of graphene allows them to be excellent electrode materials for fabricating various sensing platforms. This review article highlights the recent advances in the development of novel graphene 2D nanomaterials-based electrochemical biosensors. There are thousands of papers published since 2012. Since the unique nanostructure and remarkable synergy effect allow them to be good electrode candidate, the graphene 2D nanomaterials have been employed in various electrochemical biosensing platforms towards the determination of glucose, H_2O_2, DNA, biomarkers and pathogens. Although considerable efforts have been made for developing promising graphene based biosensors, the investigation of their practical applications in real samples is still at the beginning. Some important issues and challenges should be addressed. Recently, some graphene-like nanomaterials, such as C_3N_4, BN, and MoS_2, etc (Pumera and Loo, 2014; Farimani et al., 2014; Huang et al., 2013c, 2013b; Hou et al., 2013), have been proposed in 2D nanomaterials based biosensors. As the class of emerging materials, graphene-like nanomaterials with specific planar morphology have attracted significant attentions. Taking the advantages of varicosity composition and diverse structural effect, these kinds of nanomaterials have promoted great efforts to improve application and reliability of electrochemical biosensors. The synthesis and functionalization of graphene-like nanomaterials with high-quality planar morphology are highly desirable. Moreover, researchers should also endeavor more effort on the hybrid real systems combining other functional nanomaterials with graphene 2D nanomaterials. For instance, the incorporation of graphene nanomaterials in microfluidics-based electrochemical biosensors needs to be further explored for detections of different analytes. Additional properties and synergistic effects involved are beneficial for the enhanced applications. Moreover, the developments of new graphene-like 2D nanomaterials with high electrochemical performances will lead to significant advance in analytic applications. Finally, graphene based materials enable us to develop miniaturized biosensing systems that could be used for simultaneous detections of multiple analytes in biomedical, environmental, food safety, and global health applications.

In order to develop more sensitive and reliable electrochemical biosensors based on graphene and graphene-like 2D nanomaterials, more efforts should be made on the synthesis and functionalization of the graphene and graphene-like materials with unique physical and chemical properties. First, novel approaches need to be investigated to effectively separate graphene layers and to prevent them from agglomeration in the process of biosensor fabrication. Besides, new techniques are needed to functionalize graphene with desirable physical, chemical, and electrical properties, including the enhanced stability of graphene in biological medium, the reduced toxicity of graphene to cell and the better selectivity of graphene based biosensor, etc.

The most important challenge of graphene 2D nanomaterials-based electrochemical biosensor is the real application, such as analysis of targets in real samples. Two issues should be clarified in this area. One is the real sample matrix influence, such as blood and plasma. Real samples always contain the mixture of molecules and ions that would produce the nonspecific signal. Generally, most reports were performed with pure analytes in buffer solutions. Therefore, researchers should also make more effort on exploring the novel biosensor designs with high selectivity in complex conditions. Secondly, the most reported graphene-based electrochemical biosensors were designed and fabricated at lab-scale and are not suitable for commercial-scale production. The electrochemical biosensors need be designed and fabricated for commercial-scale production with good reproducibility and low cost. We expect that future innovative research on graphene 2D nanomaterials will couple with other major technological advance, such as lateral-flow, lab-on-chip, and 3D printing techniques for the development of next-generation biosensors.

Acknowledgments

This work was supported partially by Grant U01 NS058161 from the National Institutes of Health Office of the Director (NIH OD), and the National Institute of Neurological Disorders and Stroke (NINDS), Grant R01 OH008173-01 from the CDC/NIOSH, and Grant U54 ES016015-010003 from the National Institute of Environmental Health Sciences (NIH). Its contents are solely the responsibility of the authors and do not necessarily represent the official views of the federal government. DD acknowledge the financial support of the National Natural Science Foundation of China (21275062) and the Program for New Century Excellent Talents in University (NCET-12-0871).

References

Akhavan, O., Ghaderi, E., Rahighi, R., 2012. ACS Nano 6, 2904–2916.
Ambrosi, A., Chua, C.K., Bonanni, A., Pumera, M., 2014. Chem. Rev. 114, 7150–7188.
Bai, L., Yan, B., Chai, Y., Yuan, R., Yuan, Y., Xie, S., Jiang, L., He, Y., 2013a. Analyst 138, 6595–6599.
Bai, L., Yuan, R., Chai, Y., Zhuo, Y., Yuan, Y., Wang, Y., 2012. Biomaterials 33, 1090–1096.
Bai, X., Chen, G., Shiu, K., 2013b. Electrochim. Acta 89, 454–460.
Benvidi, A., Rajabzadeh, N., Mazloum-Ardakani, M., Heidari, M.M., Mulchandani, A., 2014. Biosens. Bioelectron. 58, 145–152.
Cai, B., Wang, S., Huang, L., Ning, Y., Zhang, Z., Zhang, G., 2014. ACS Nano 8, 2632–2638.
Cai, Y., Li, H., Li, Y., Zhao, Y., Ma, H., Zhu, B., Xu, C., Wei, Q., Wu, D., Du, B., 2012. Biosens. Bioelectron. 36, 6–11.
Cao, S., Zhang, L., Chai, Y., Yuan, R., 2013a. Biosens. Bioelectron. 42, 532–538.
Cao, X., Ye, Y., Li, Y., Xu, X., Yu, J., Liu, S., 2013b. J. Electroanal. Chem. 697, 10–14.
Chen, A., Chatterjee, S., 2013. Chem. Soc. Rev. 42, 5425–5438.
Chen, D., Feng, H., Li, J., 2012a. Chem. Rev. 112, 6027–6053.
Chen, H., Tang, D., Zhang, B., Liu, B., Cui, Y., Chen, G., 2012b. Talanta 91, 95–102.
Chen, J., Zheng, X., Miao, F., Zhang, J., Cui, X., Zheng, W., 2012c. J. Appl. Electrochem. 42, 875–881.
Chen, J.R., Jiao, X.X., Luo, H.Q., Li, N.B., 2013a. J. Mater. Chem. B 1, 861–864.
Chen, X., Jia, X., Han, J., Ma, J., Ma, Z., 2013b. Biosens. Bioelectron. 50, 356–361.
Chen, Y., Tan, C., Zhang, H., Wang, L., 2015. Chem. Soc. Rev. 44, 2681–2701.
Cheng, S., Hotani, K., Hideshima, S., Kuroiwa, S., Nakanishi, T., Hashimoto, M., Mori, Y., Osaka, T., 2014. Materials 7, 2490–2500.
Claussen, J.C., Kumar, A., Jaroch, D.B., Khawaja, M.H., Hibbard, A.B., Porterfield, D.M., Fisher, T.S., 2012. Adv. Funct. Mater. 22, 3399–3405.
Dong, X., Xu, H., Wang, X., Huang, Y., Chan-Park, M.B., Zhang, H., Wang, L., Huang, W., Chen, P., 2012a. ACS Nano 6, 3206–3213.
Dong, H., Zhu, Z., Ju, H., Yan, F., 2012b. Biosens. Bioelectron. 33, 228–232.
Dresselhaus, M.S., Araujo, P.T., 2010. ACS Nano 4, 6297–6302.
Du, D., Wang, L., Shao, Y., Wang, J., Engelhard, M.H., Lin, Y., 2011. Anal. Chem. 83, 746–752.
Du, D., Yang, Y., Lin, Y., 2012. MRS Bull. 37, 1290–1296.
Du, D., Guo, S., Tang, L., Ning, Y., Yao, Q., Zhang, G., 2013. Sens. Actuators B 186, 563–570.
Eissa, S., Tlili, C., L'Hocine, L., Zourob, M., 2012. Biosens. Bioelectron. 38, 308–313.

Esteban-Fernández de Ávila, B., Araque, E., Campuzano, S., Pedrero, M., Dalkiran, B., Barderas, R., Villalonga, R., Kiliç, E., Pingarrón, J.M., 2015. Anal. Chem. 87, 2290–2298.
Fan, Z., Lin, Q., Gong, P., Liu, B., Wang, J., Yang, S., 2015. Electrochim. Acta 151, 186–194.
Fang, Y., Wang, E., 2013. Chem. Commun. 49, 9526–9539.
Farimani, A.B., Min, K., Aluru, N.R., 2014. ACS Nano 8, 7914–7922.
Feng, D., Li, L., Han, X., Fang, X., Li, X., Zhang, Y., 2014. Sens. Actuators B 201, 360–368.
Freedman, K.J., Ahn, C.W., Kim, M.J., 2013. ACS Nano 7, 5008–5016.
Gai, P., Zhao, C., Wang, Y., Abdel-Halim, E.S., Zhang, J., Zhu, J., 2014. Biosens. Bioelectron. 62, 170–176.
Gao, L., Lian, C., Zhou, Y., Yan, L., Li, Q., Zhang, C., Chen, L., Chen, K., 2014a. Biosens. Bioelectron. 60, 22–29.
Gao, Y., Xu, J., Lu, L., Wu, L., Zhang, K., Nie, T., Zhu, X., Wu, Y., 2014b. Biosens. Bioelectron. 62, 261–267.
Gasnier, A., Laura Pedano, M., Rubianes, M.D., Rivas, G.A., 2013. Sens. Actuators B 176, 921–926.
Ge, S., Sun, M., Liu, W., Li, S., Wang, X., Chu, C., Yan, M., Yu, J., 2014. Sens. Actuators B 192, 317–326.
Ge, S., Yan, M., Lu, J., Zhang, M., Yu, F., Yu, J., Song, X., Yu, S., 2012. Biosens. Bioelectron. 31, 49–54.
Geim, A.K., 2009. Science 324, 1530–1534.
Gholivand, M.B., Khodadadian, M., 2014. Biosens. Bioelectron. 53, 472–478.
Goenka, S., Sant, V., Sant, S., 2014. J. Control. Release 173, 75–88.
Goran, J.M., Mantilla, S.M., Stevenson, K.J., 2013. Anal. Chem. 85, 1571–1581.
Govindhan, M., Amiri, M., Chen, A., 2015. Biosens. Bioelectron. 66, 474–480.
Gu, H., Yang, Y., Zhou, X., Zhou, T., Shi, G., 2014. J. Electroanal. Chem. 730, 41–47.
Gu, H., Yu, Y., Liu, X., Ni, B., Zhou, T., Shi, G., 2012. Biosens. Bioelectron. 32, 118–126.
Guo, S., Du, D., Tang, L., Ning, Y., Yao, Q., Zhang, G., 2013a. Analyst 138, 3216–3220.
Guo, Y., Guo, Y., Dong, C., 2013b. Electrochim. Acta 113, 69–76.
Guo, Y., Wang, Y., Liu, S., Yu, J., Wang, H., Cui, M., Huang, J., 2015. Analyst 140, 551–559.
Han, J., Ma, J., Ma, Z., 2013. Biosens. Bioelectron. 47, 243–247.
Haque, A.J., Park, H., Sung, D., Jon, S., Choi, S., Kim, K., 2012. Anal. Chem. 84, 1871–1878.
Hasanzadeh, M., Shadjou, N., Eskandani, M., de la Guardia, M., Omidinia, E., 2013. TrAC Trends Anal. Chem. 49, 20–30.
He, R.X., Lin, P., Liu, Z.K., Zhu, H.W., Zhao, X.Z., Chan, H.L.W., Yan, F., 2012. Nano Lett. 12, 1404–1409.
Hou, Y., Wen, Z., Cui, S., Guo, X., Chen, J., 2013. Adv. Mater. 25, 6291–6297.
Hu, Y., Li, F., Han, D., Wu, T., Zhang, Q., Niu, L., Bao, Y., 2012a. Anal. Chim. Acta 753, 82–89.
Hu, Y., Wang, K., Zhang, Q., Li, F., Wu, T., Niu, L., 2012b. Biomaterials 33, 1097–1106.
Huang, J., Tian, J., Zhao, Y., Zhao, S., 2015. Sens. Actuators B 206, 570–576.
Huang, J., Zhang, L., Liang, R., Qiu, J., 2013a. Biosens. Bioelectron. 41, 430–435.
Huang, K., Liu, Y., Wang, H., Wang, Y., 2014. Electrochim. Acta 118, 130–137.
Huang, X., Zeng, Z., Bao, S., Wang, M., Qi, X., Fan, Z., Zhang, H., 2013b. Nat. Commun. 4, 1444.
Huang, X., Zeng, Z., Zhang, H., 2013c. Chem. Soc. Rev. 42, 1934–1946.
Hui, J., Cui, J., Xu, G., Adeloju, S.B., Wu, Y., 2013. Mater. Lett. 108, 88–91.
Jang, H.D., Kim, S.K., Chang, H., Roh, K., Choi, J., Huang, J., 2012. Biosens. Bioelectron. 38, 184–188.
Jang, H., Ahn, J., Kim, M., Shin, Y., Jeun, M., Cho, W., Lee, K.H., 2015. Biosens. Bioelectron. 64, 318–323.
Jayakumar, K., Rajesh, R., Dharuman, V., Venkatasan, R., Hahn, J.H., Karutha Pandian, S., 2012. Biosens. Bioelectron. 31, 406–412.
Jia, L., Liu, J., Wang, H., 2015. Biosens. Bioelectron. 67, 139–145.
Jiang, J., Fan, W., Du, X., 2014. Biosens. Bioelectron. 51, 343–348.
Jiang, S., Hua, E., Liang, M., Liu, B., Xie, G., 2013. Colloids Surf. B 101, 481–486.
Jin, B., Wang, P., Mao, H., Hu, B., Zhang, H., Cheng, Z., Wu, Z., Bian, X., Jia, C., Jing, F., Jin, Q., Zhao, J., 2014. Biosens. Bioelectron. 55, 464–469.
Kamat, P.V., 2010. J. Phys. Chem. Lett. 1, 520–527.
Kang, J., Korecka, M., Toledo, J.B., Trojanowski, J.Q., Shaw, L.M., 2013. Clin. Chem. 59, 903–916.
Kang, X., Wang, J., Wu, H., Aksay, I.A., Liu, J., Lin, Y., 2009. Biosens. Bioelectron. 25, 901–905.
Kavitha, T., Gopalan, A.I., Lee, K., Park, S., 2012. Carbon 50, 2994–3000.
Kong, F., Gu, S., Li, W., Chen, T., Xu, Q., Wang, W., 2014. Biosens. Bioelectron. 56, 77–82.
Kong, F., Xu, B., Du, Y., Xu, J., Chen, H., 2013. Chem. Commun. 49, 1052–1054.
Lai, G., Zhang, H., Tamanna, T., Yu, A., 2014. Anal. Chem. 86, 1789–1793.
Lai, Y., Bai, J., Shi, X., Zeng, Y., Xian, Y., Hou, J., Jin, L., 2013. Talanta 107, 176–182.
Lawal, A.T., 2015. Talanta 131, 424–443.
Li, D., Liu, J., Barrow, C.J., Yang, W., 2014a. Chem. Commun. 50, 8197–8200.
Li, D., Kaner, R.B., 2008. Science 320, 1170–1171.
Li, H., He, J., Li, S., Turner, A.P.F., 2013a. Biosens. Bioelectron. 43, 25–29.
Li, H., Wei, Q., He, J., Li, T., Zhao, Y., Cai, Y., Du, B., Qian, Z., Yang, M., 2011. Biosens. Bioelectron. 26, 3590–3595.
Li, P., Chen, X., Yang, W., 2013b. Langmuir 29, 8629–8635.
Li, Y., Xu, C., Li, H., Wang, H., Wu, D., Ma, H., Cai, Y., Du, B., Wei, Q., 2014b. Biosens. Bioelectron. 56, 295–299.
Li, Z., Wang, Y., Wang, J., Tang, Z., Pounds, J.G., Lin, Y., 2010. Anal. Chem. 82, 7008–7014.
Li, Z., Xie, C., Wang, J., Meng, A., Zhang, F., 2015. Sens. Actuators B. 208, 505–511.
Li, Z., Huang, Y., Chen, L., Qin, X., Huang, Z., Zhou, Y., Meng, Y., Li, J., Huang, S., Liu, Y., Wang, W., Xie, Q., Yao, S., 2013c. Sens. Actuators B. 181, 280–287.
Liang, B., Fang, L., Yang, G., Hu, Y., Guo, X., Ye, X., 2013. Biosens. Bioelectron. 43, 131–136.
Liang, B., Guo, X., Fang, L., Hu, Y., Yang, G., Zhu, Q., Wei, J., Ye, X., 2015. Electrochem. Commun. 50, 1–5.
Lin, C., Wei, K., Liao, S., Huang, C., Sun, C., Wu, P., Lu, Y., Yang, H., Ma, C.M., 2015. Biosens. Bioelectron. 67, 431–437.
Lin, D., Wu, J., Ju, H., Yan, F., 2014. Biosens. Bioelectron. 52, 153–158.
Lin, D., Wu, J., Wang, M., Yan, F., Ju, H., 2012. Anal. Chem. 84, 3662–3668.
Lin, J., Wei, Z., Zhang, H., Shao, M., 2013. Biosens. Bioelectron. 41, 342–347.
Liu, B., Du, D., Hua, X., Yu, X., Lin, Y., 2014a. Electroanalysis 26, 1214–1223.
Liu, F., Zhang, Y., Ge, S., Lu, J., Yu, J., Song, X., Liu, S., 2012a. Talanta 99, 512–519.
Liu, J., Wang, J., Wang, T., Li, D., Xi, F., Wang, J., Wang, E., 2015a. Biosens. Bioelectron. 65, 281–286.
Liu, S., Tian, J., Wang, L., Luo, Y., Lu, W., Sun, X., 2011. Biosens. Bioelectron. 26, 4491–4496.
Liu, X., Zhang, J., Yan, R., Zhang, Q., Liu, X., 2014b. Biosens. Bioelectron. 51, 76–81.
Liu, Y., Liu, Y., Feng, H., Wu, Y., Joshi, L., Zeng, X., Li, J., 2012b. Biosens. Bioelectron. 35, 63–68.
Liu, Y., Dong, X., Chen, P., 2012c. Chem. Soc. Rev. 41, 2283.
Liu, Z., Guo, Y., Dong, C., 2015b. Talanta 137, 87–93.
Lu, L., Li, H., Qu, F., Zhang, X., Shen, G., Yu, R., 2011a. Biosens. Bioelectron. 26, 3500–3504.
Lu, L., Qiu, X., Zhang, X., Shen, G., Tan, W., Yu, R., 2013. Biosens. Bioelectron. 45, 102–107.
Lu, W., Luo, Y., Chang, G., Sun, X., 2011b. Biosens. Bioelectron. 26, 4791–4797.
Lu, Y., Lerner, M.B., John Qi, Z., Mitala, J.J., Hsien Lim, J., Discher, B.M., Charlie Johnson, A.T., 2012. Appl. Phys. Lett. 100, 033110.
Luo, L., Zhang, Z., Ding, Y., Deng, D., Zhu, X., Wang, Z., 2013. Nanoscale 5, 5833–5840.
Lv, W., Guo, M., Liang, M., Jin, F., Cui, L., Zhi, L., Yang, Q., 2010. J. Mater. Chem. 20, 6668–6673.
Mao, H.Y., Laurent, S., Chen, W., Akhavan, O., Imani, M., Ashkarran, A.A., Mahmoudi, M., 2013. Chem. Rev. 113, 3407–3424.
Mao, K., Wu, D., Li, Y., Ma, H., Ni, Z., Yu, H., Luo, C., Wei, Q., Du, B., 2012. Anal. Biochem. 422, 22–27.
Martín, A., Hernández-Ferrer, J., Martínez, M.T., Escarpa, A., 2015. Electrochim. Acta 172, 2–6.
Muthurasu, A., Ganesh, V., 2014. Appl. Biochem. Biotechnol. 174, 945–959.
Nguyen, P., Berry, V., 2012. J. Phys. Chem. Lett. 3, 1024–1029.
Niu, S., Sun, J., Nan, C., Lin, J., 2013. Sens. Actuators B 176, 58–63.
Okamoto, S., Ohno, Y., Maehashi, K., Inoue, K., Matsumoto, K., 2012. Jpn. J. Appl. Phys. 51, 06FD08.
Park, J.W., Lee, C., Jang, J., 2015. Sens. Actuators B 208, 532–537.
Park, J.S., Baek, A., Park, I., Jun, B., Kim, D., 2013. Chem. Commun. 49, 9203–9205.
Park, S., Singh, A., Kim, S., Yang, H., 2014. Anal. Chem. 86, 1560–1566.
Ping, J., Zhou, Y., Wu, Y., Papper, V., Boujday, S., Marks, R.S., Steele, T.W.J., 2015. Biosens. Bioelectron. 64, 373–385.
Premkumar, T., Geckeler, K.E., 2012. Prog. Polym. Sci. 37, 515–529.
Pumera, M., 2012. Electrochemistry of graphene-based nanomaterials. In: Graphite, Graphene, and Their Polymer Nanocomposites, Prithu Mukhopadhyay, Rakesh K. Gupta (Eds.) CRC Press, Boca Raton, FL, pp. 263–282.
Pumera, M., 2010. Chem. Soc. Rev. 39, 4146–4157.
Pumera, M., Ambrosi, A., Bonanni, A., Chng, E.L.K., Poh, H.L., 2010. TrAC Trends Anal. Chem. 29, 954–965.
Pumera, M., Loo, A.H., 2014. TrAC Trends Anal. Chem. 61, 49–53.
Puster, M., Rodríguez-Manzo, J.A., Balan, A., Drndić, M., 2013. ACS Nano 7, 11283–11289.
Putzbach, W., Ronkainen, N.J., 2013. Sensors 13, 4811–4840.
Qi, P., Wan, Y., Zhang, D., 2013. Biosens. Bioelectron. 39, 282–288.
Qi, T., Liao, J., Li, Y., Peng, J., Li, W., Chu, B., Li, H., Wei, Y., Qian, Z., 2014. Biosens. Bioelectron. 61, 245–250.
Ramakrishna Matte, H.S.S., Gomathi, A., Manna, A.K., Late, D.J., Datta, R., Pati, S.K., Rao, C.N.R., 2010. Angew. Chem. 122, 4153–4156.
Rasheed, P.A., Sandhyarani, N., 2014. Sens. Actuators B 204, 777–782.
Razmi, H., Mohammad-Rezaei, R., 2013. Biosens. Bioelectron. 41, 498–504.
Ruan, C., Shi, W., Jiang, H., Sun, Y., Liu, X., Zhang, X., Sun, Z., Dai, L., Ge, D., 2013. Sens. Actuators B 177, 826–832.
Ruecha, N., Rangkupan, R., Rodthongkum, N., Chailapakul, O., 2014. Biosens. Bioelectron. 52, 13–19.
Rusling, J.F., 2013. Anal. Chem. 85, 5304–5310.
Salavagione, H.J., Martínez, G., Ellis, G., 2011. Macromol. Rapid Commun. 32, 1771–1789.
Sanghavi, B.J., Sitaula, S., Griep, M.H., Karna, S.P., Ali, M.F., Swami, N.S., 2013. Anal. Chem. 85, 8158–8165.
Schneider, G.F., Xu, Q., Hage, S., Luik, S., Spoor, J.N.H., Malladi, S., Zandbergen, H., Dekker, C., 2013. Nat. Commun. 4.
Seehuber, A., Dahint, R., 2013. J. Phys. Chem. B 117, 6980–6989.
Shan, C., Yang, H., Han, D., Zhang, Q., Ivaska, A., Niu, L., 2010. Biosens. Bioelectron. 25, 1070–1074.
Sharma, P., Tuteja, S.K., Bhalla, V., Shekhawat, G., Dravid, V.P., Suri, C.R., 2013. Biosens. Bioelectron. 39, 99–105.
Shen, G., Hu, X., Zhang, S., 2014a. J. Electroanal. Chem 717–718, 172–176.
Shen, J., Li, Y., Gu, H., Xia, F., Zuo, X., 2014b. Chem. Rev. 114, 7631–7677.
Shi, F., Zheng, W., Wang, W., Hou, F., Lei, B., Sun, Z., Sun, W., 2015. Biosens. Bioelectron. 64, 131–137.

Shi, J., He, T., Jiang, F., Abdel-Halim, E.S., Zhu, J., 2014. Biosens. Bioelectron. 55, 51–56.
Shiddiky, M.J.A., Rauf, S., Kithva, P.H., Trau, M., 2012. Biosens. Bioelectron. 35, 251–257.
Singal, S., Srivastava, A.K., Biradar, A.M., Mulchandani, A., Rajesh, 2014. Sens. Actuators B. 205, 363–370.
Song, Y., Liu, H., Tan, H., Xu, F., Jia, J., Zhang, L., Li, Z., Wang, L., 2014. Anal. Chem. 86, 1980–1987.
Song, Y., Liu, H., Wan, L., Wang, Y., Hou, H., Wang, L., 2013a. Electroanalysis 25, 1400–1409.
Song, Y., Liu, H., Wang, Y., Wang, L., 2013b. Electrochim. Acta 93, 17–24.
Sun, W., Guo, Y., Ju, X., Zhang, Y., Wang, X., Sun, Z., 2013. Biosens. Bioelectron. 42, 207–213.
Sun, W., Qi, X., Zhang, Y., Yang, H., Gao, H., Chen, Y., Sun, Z., 2012a. Electrochim. Acta 85, 145–151.
Sun, W., Zhang, Y., Ju, X., Li, G., Gao, H., Sun, Z., 2012b. Anal. Chim. Acta 752, 39–44.
Taleat, Z., Cristea, C., Marrazza, G., Mazloum-Ardakani, M., Săndulescu, R., 2014. J. Electroanal. Chem. 717–718, 119–124.
Tan, S.M., Sofer, Z., Pumera, M., 2013. Electroanalysis 25, 703–705.
Tang, J., Tang, D., Niessner, R., Chen, G., Knopp, D., 2011. Anal. Chem. 83, 5407–5414.
Tang, S., Tong, P., Lu, W., Chen, J., Yan, Z., Zhang, L., 2014. Biosens. Bioelectron. 59, 1–5.
Tang, Z., Wu, H., Cort, J.R., Buchko, G.W., Zhang, Y., Shao, Y., Aksay, I.A., Liu, J., Lin, Y., 2010. Small 6, 1205–1209.
Teymourian, H., Salimi, A., Khezrian, S., 2013. Biosens. Bioelectron. 49, 1–8.
Tiwari, I., Singh, M., Pandey, C.M., Sumana, G., 2015. Sens. Actuators B 206, 276–283.
Tran, H.V., Piro, B., Reisberg, S., Duc, H.T., Pham, M.C., 2013. Anal. Chem. 85, 8469–8474.
Traversi, F., Raillon, C., Benameur, S.M., Liu, K., Khlybov, S., Tosun, M., Krasnozhon, D., Kis, A., Radenovic, A., 2013. Nat. Nanotechnol. 8, 939–945.
Vashist, S.K., Luong, J.H.T., 2015. Carbon 84, 519–550.
Vilela, D., Orozco, J., Cheng, G., Sattayasamitsathit, S., Galarnyk, M., Kan, C., Wang, J., Escarpa, A., 2014. Lab Chip 14, 3505–3509.
Walcarius, A., Minteer, S.D., Wang, J., Lin, Y., Merkoci, A., 2013. J. Mater. Chem. B 1, 4878–4908.
Wan, Y., Su, Y., Zhu, X., Liu, G., Fan, C., 2013. Biosens. Bioelectron. 47, 1–11.
Wang, Y., Yao, Y., 2012. Microchim. Acta 176, 271–277.
Wang, B., Chang, Y., Zhi, L., 2011a. New Carbon Mater. 26, 31–35.
Wang, G., Gang, X., Zhou, X., Zhang, G., Huang, H., Zhang, X., Wang, L., 2013a. Talanta 103, 75–80.
Wang, G., He, X., Chen, L., Zhu, Y., Zhang, X., 2014a. Colloids Surf. B 116, 714–719.
Wang, G., Qian, Y., Cao, X., Xia, X., 2012a. Electrochem. Commun. 20, 1–3.
Wang, H., Wang, J., Timchalk, C., Lin, Y., 2008. Anal. Chem. 80, 8477–8484.
Wang, J., 2006. Biosens. Bioelectron. 21, 1887–1892.
Wang, K., Liu, Q., Guan, Q., Wu, J., Li, H., Yan, J., 2011b. Biosens. Bioelectron. 26, 2252–2257.
Wang, L., Hua, E., Liang, M., Ma, C., Liu, Z., Sheng, S., Liu, M., Xie, G., Feng, W., 2014b. Biosens. Bioelectron. 51, 201–207.
Wang, Q., Su, J., Xu, J., Xiang, Y., Yuan, R., Chai, Y., 2012b. Sens. Actuators B 163, 267–271.
Wang, Q., Lei, J., Deng, S., Zhang, L., Ju, H., 2013b. Chem. Commun. 49, 916–918.
Wang, Y., Li, H., Kong, J., 2014c. Sens. Actuators B 193, 708–714.
Wang, Y., Shao, Y., Matson, D.W., Li, J., Lin, Y., 2010. ACS Nano 4, 1790–1798.
Wang, Y., Tang, L., Li, Z., Lin, Y., Li, J., 2014d. Nat. Protoc. 9, 1944–1955.
Wang, Y., Ping, J., Ye, Z., Wu, J., Ying, Y., 2013c. Biosens. Bioelectron. 49, 492–498.
Wang, Z., Zhang, J., Yin, Z., Wu, S., Mandler, D., Zhang, H., 2012c. Nanoscale 4, 2728–2733.
Wei, Q., Zhao, Y., Du, B., Wu, D., Li, H., Yang, M., 2012. Food Chem. 134, 1601–1606.
Wen, J., Zhou, S., Yuan, Y., 2014. Biosens. Bioelectron. 52, 44–49.
Wen, W., Chen, W., Ren, Q., Hu, X., Xiong, H., Zhang, X., Wang, S., Zhao, Y., 2012. Sens. Actuators B. 166–167, 444–450.
Wooten, M., Karra, S., Zhang, M., Gorski, W., 2014. Anal. Chem. 86, 752–757.
Wu, H., Wang, J., Kang, X., Wang, C., Wang, D., Liu, J., Aksay, I.A., Lin, Y., 2009. Talanta 80, 403–406.
Wu, L., Xiong, E., Zhang, X., Zhang, X., Chen, J., 2014a. Nano Today 9, 197–211.
Wu, S., He, Q., Tan, C., Wang, Y., Zhang, H., 2013a. Small 9, 1160–1172.
Wu, S., Lan, X., Huang, F., Luo, Z., Ju, H., Meng, C., Duan, C., 2012. Biosens. Bioelectron. 32, 293–296.
Wu, Y., Xue, P., Hui, K.M., Kang, Y., 2014b. Biosens. Bioelectron. 52, 180–187.
Wu, Y., Xue, P., Kang, Y., Hui, K.M., 2013b. Anal. Chem. 85, 3166–3173.
Wu, Y., Xue, P., Kang, Y., Hui, K.M., 2013c. Anal. Chem. 85, 8661–8668.
Xiang, Q., Yu, J., Jaroniec, M., 2012. J. Am. Chem. Soc. 134, 6575–6578.
Xie, L., Xu, Y., Cao, X., 2013. Colloids Surf. B 107, 245–250.
Xie, S., Chai, Y., Yuan, R., Bai, L., Yuan, Y., Wang, Y., 2012. Anal. Chim. Acta 755, 46–53.
Xie, Y., Chen, A., Du, D., Lin, Y., 2011. Anal. Chim. Acta 699, 44–48.
Xu, Q., Gu, S., Jin, L., Zhou, Y., Yang, Z., Wang, W., Hu, X., 2014. Sens. Actuators B 190, 562–569.
Xu, Q., Wang, L., Lei, J., Deng, S., Ju, H., 2013. J. Mater. Chem. B 1, 5347–5352.
Yan, J., Ge, L., Song, X., Yan, M., Ge, S., Yu, J., 2012. Chem. Eur. J. 18, 4938–4945.
Yang, G., Cao, J., Li, L., Rana, R.K., Zhu, J., 2013a. Carbon 51, 124–133.
Yang, G., Li, L., Rana, R.K., Zhu, J., 2013b. Carbon 61, 357–366.
Yang, M., Javadi, A., Gong, S., 2011a. Sens. Actuators B 155, 357–360.
Yang, T., Guan, Q., Guo, X., Meng, L., Du, M., Jiao, K., 2013c. Anal. Chem. 85, 1358–1366.
Yang, T., Li, Q., Meng, L., Wang, X., Chen, W., Jiao, K., 2013d. ACS Appl. Mater. Interfaces 5, 3495–3499.
Yang, T., Meng, L., Wang, X., Wang, L., Jiao, K., 2013e. ACS Appl. Mater. Interfaces 5, 10889–10894.
Yang, T., Meng, L., Zhao, J., Wang, X., Jiao, K., 2014. ACS Appl. Mater. Interfaces 6, 19050–19056.
Yang, Y., Dong, S., Shen, T., Jian, C., Chang, H., Li, Y., Zhou, J., 2011b. Electrochim. Acta 56, 6021–6025.
Yang, Y., Asiri, A.M., Tang, Z., Du, D., Lin, Y., 2013f. Mater. Today 16, 365–373.
Yang, Z., Zhuo, Y., Yuan, R., Chai, Y., 2015. Biosens. Bioelectron. 69, 321–327.
Yetisen, A.K., Akram, M.S., Lowe, C.R., 2013. Lab Chip 13, 2210–2251.
Yin, H., Zhou, Y., Zhang, H., Meng, X., Ai, S., 2012. Biosens. Bioelectron. 33, 247–253.
Yoon, H., Jang, J., 2009. Adv. Funct. Mater. 19, 1567–1576.
Yu, L., Lee, Y., Ling, X., Santos, E.J.G., Shin, Y.C., Lin, Y., Dubey, M., Kaxiras, E., Kong, J., Wang, H., Palacios, T., 2014a. Nano Lett. 14, 3055–3063.
Yu, S., Wei, Q., Du, B., Wu, D., Li, H., Yan, L., Ma, H., Zhang, Y., 2013. Biosens. Bioelectron. 48, 224–229.
Yu, Y., Chen, Z., He, S., Zhang, B., Li, X., Yao, M., 2014b. Biosens. Bioelectron. 52, 147–152.
Yuan, Y., Liu, G., Yuan, R., Chai, Y., Gan, X., Bai, L., 2013. Biosens. Bioelectron. 42, 474–480.
Yue, H.Y., Huang, S., Chang, J., Heo, C., Yao, F., Adhikari, S., Gunes, F., Liu, L.C., Lee, T. H., Oh, E.S., Li, B., Zhang, J.J., Huy, T.Q., Luan, N.V., Lee, Y.H., 2014. ACS Nano 8, 1639–1646.
Zeng, Q., Cheng, J., Liu, X., Bai, H., Jiang, J., 2011. Biosens. Bioelectron. 26, 3456–3463.
Zhang, J., Chen, X., Yang, M., 2014a. Sens. Actuators B 196, 189–193.
Zhang, L., Han, G., Liu, Y., Tang, J., Tang, W., 2014b. Sens. Actuators B 197, 164–171.
Zhang, N., Lv, X., Ma, W., Hu, Y., Li, F., Han, D., Niu, L., 2013. Talanta 107, 195–202.
Zhang, P., Zhao, X., Ji, Y., Ouyang, Z., Wen, X., Li, J., Su, Z., Wei, G., 2015a. J. Mater. Chem. B 3, 2487–2496.
Zhang, Q., Wu, S., Zhang, L., Lu, J., Verproot, F., Liu, Y., Xing, Z., Li, J., Song, X., 2011. Biosens. Bioelectron. 26, 2632–2637.
Zhang, W., Asiri, A.M., Liu, D., Du, D., Lin, Y., 2014c. TrAC Trends Anal. Chem. 54, 1–10.
Zhang, X., Liao, Q., Chu, M., Liu, S., Zhang, Y., 2014d. Biosens. Bioelectron. 52, 281–287.
Zhang, Y., Zeng, G.M., Tang, L., Chen, J., Zhu, Y., He, X.X., He, Y., 2015b. Anal. Chem. 87, 989–996.
Zhang, Z., Luo, L., Chen, G., Ding, Y., Deng, D., Fan, C., 2014e. Biosens. Bioelectron. 60, 161–166.
Zhao, W., Xu, J., Chen, H., 2014. Chem. Rev. 114, 7421–7441.
Zhong, X., Yuan, R., Chai, Y., 2012. Sens. Actuators B 162, 334–340.
Zhong, Z., Li, M., Qing, Y., Dai, N., Guan, W., Liang, W., Wang, D., 2014. Analyst 139, 6563–6568.
Zhou, J., Lu, Q., Tong, Y., Wei, W., Liu, S., 2012a. Talanta 99, 625–630.
Zhou, K., Zhu, Y., Yang, X., Li, C., 2010. Electroanalysis 22, 259–264.
Zhou, Y., Yin, H., Meng, X., Xu, Z., Fu, Y., Ai, S., 2012b. Electrochim. Acta 71, 294–301.
Zhu, C., Dong, S., 2014. Electroanalysis 26, 14–29.
Zhu, C., Yang, G., Li, H., Du, D., Lin, Y., 2015a. Anal. Chem. 87, 230–249.
Zhu, L., Luo, L., Wang, Z., 2012. Biosens. Bioelectron. 35, 507–511.
Zhu, Q., Chai, Y., Yuan, R., Zhuo, Y., Han, J., Li, Y., Liao, N., 2013a. Biosens. Bioelectron. 43, 440–445.
Zhu, Q., Chai, Y., Zhuo, Y., Yuan, R., 2015b. Biosens. Bioelectron. 68, 42–48.
Zhu, X., Sun, L., Chen, Y., Ye, Z., Shen, Z., Li, G., 2013b. Biosens. Bioelectron. 47, 32–37.
Zhu, Y., Murali, S., Cai, W., Li, X., Suk, J.W., Potts, J.R., Ruoff, R.S., 2010. Adv. Mater. 22, 3906–3924.
Zou, Z., Du, D., Wang, J., Smith, J.N., Timchalk, C., Li, Y., Lin, Y., 2010. Anal. Chem. 82, 5125–5133.